NASA Technical Memorandum 101059

In-Flight Simulation Investigation of Rotorcraft Pitch-Roll Cross Coupling

Douglas C. Watson and William S. Hindson

December 1988

NASA

National Aeronautics and
Space Administration

NASA Technical Memorandum 101059

In-Flight Simulation Investigation of Rotorcraft Pitch-Roll Cross Coupling

Douglas C. Watson
William S. Hindson, Ames Research Center, Moffett Field, California

December 1988

National Aeronautics and
Space Administration

Ames Research Center
Moffett Field, California 94035

SUMMARY

An in-flight simulation experiment investigating the handling qualities effects of pitch-roll cross-coupling characteristic of single-main-rotor helicopters is described. The experiment was conducted using the NASA/Army CH-47B variable stability helicopter with an explicit-model-following control system. The research is an extension of an earlier ground-based investigation conducted on the NASA Ames Research Center's Vertical Motion Simulator. The model developed for the experiment is for an unaugmented helicopter with cross-coupling implemented using physical rotor parameters. The details of converting the model from the simulation to use in flight are described. A frequency-domain comparison of the model and actual aircraft responses showing the fidelity of the in-flight simulation is described. The evaluation task was representative of nap-of-the-Earth maneuvering flight. The results indicate that task demands are important in determining allowable levels of coupling. In addition, on-axis damping characteristics influence the frequency-dependent characteristics of coupling and affect the handling qualities. Pilot technique, in terms of learned control crossfeeds, can improve performance and lower workload for particular types of coupling. The results obtained in flight corroborated the simulation results.

INTRODUCTION

In-flight simulation provides a valuable opportunity to validate and supplement handling qualities results obtained in ground-based simulation. In addition, the authenticity of simulator flight-evaluation tasks and corresponding pilot control techniques can be verified with full-fidelity motion and visual cues. This paper describes a flight experiment studying the effects of pitch-roll cross coupling for near-terrain flight in support of future handling qualities specifications. The flight investigation is an extension of a piloted, ground-based simulation experiment of the same subject previously conducted on the NASA Ames Research Center's Vertical Motion Simulator (VMS) (ref. 1). Accordingly, the objectives of this flight experiment were to

1. Provide new data on the effects of pitch-roll coupling typical of single-main-rotor helicopters in terrain flight;
2. Validate the previous cross-coupling simulation's handling qualities results; and
3. Identify, resolve, and document the issues involved in implementing coupled aircraft models from the simulator in the variable stability helicopter.

The assistance of Michelle Eshow, as systems operator, and George Tucker, as safety pilot, is gratefully acknowledged.

BACKGROUND

Cross coupling is generally acknowledged to be a limiting factor on the ability of a pilot to exploit the full maneuvering capability of rotorcraft. However, little research has been focused on the effects of cross coupling on rotorcraft handling qualities. A major difficulty in studying the subject lies in characterizing and quantifying pitch-roll coupling in a realistic and pertinent manner. This problem has been approached by researchers in various ways. The rest of this section will describe the general approaches taken in previous experimental and analytical research programs.

The effects of cyclic control cross-coupling were investigated by Garren (ref. 2). The cross-control phase angle, defined as the "angle through which the pilot must cross-control to obtain a pure (pitch or roll) response" was the primary experimental variable. This investigation was conducted using a variable-stability helicopter that also allowed adjustment of the pitch and roll control sensitivities and rate damping. Cross-control phase angles of less than 20° were found to have little effect, and angles of greater than 35° were considered to be unsatisfactory.

In reference 3, Chen used physical rotor parameters to effect changes in both control coupling and angular-rate coupling. The fixed-base simulation experiment used a nine-degree-of-freedom mathematical model which included rotor flapping and coning modes. The basic rotor parameters varied were pitch-flap coupling, real or effective hinge offset, flapping stiffness, and rotor lock number. Teetering, articulated and hingeless rotor configurations were considered and coupling effects were varied for each. The results of the experiment indicated that "even very high values of angular-rate coupling (M_p, L_q) did not necessarily degrade pilot ratings." Instead, "the ratios L_q/L_p and M_p/M_q appeared to be more important than the values of the coupling terms themselves." For $|L_q/L_p|$ greater than 0.35 the pilot ratings were unsatisfactory, whereas ratios less than 0.25 went unnoticed.

The $|L_q/L_p| = |M_p/M_q|$ ratio was also used by Corliss and Carico (ref. 4) for quantifying cross coupling. In this case, the test facility was a variable-stability helicopter. Changes in control sensitivity, damping, and control and angular-rate coupling were investigated. The results corroborated those of reference 3. The authors also suggested, however, that the frequency-dependent aspects of cross-coupling should be investigated.

White and Blake (ref. 5) characterized cross-coupling analytically in terms of the frequency response. They plotted "the amplitude ratios of the commanded response and the cross axis response along with the ratio of the unwanted response to the commanded response." The term "response ratio" refers to this ratio of unwanted to commanded response. This paper also proposed a simplified model for dynamic inflow that correlated well with flight test results. This inflow effect was shown to cause substantial changes in low-speed stability derivatives governing longitudinal-lateral coupling.

Chen, in an analytical study (ref. 6), showed that pitch-flap coupling (fig. 1) is an effective tool for decoupling the flapping contributions to pitch and roll rate coupling. The first-order dynamic inflow model developed in reference 5 was used in the analysis. Perfect decoupling is possible in hover and is shown to be effective for advance ratios up to 0.3.

As noted in the introduction, this current work is an extension of a piloted ground-simulation study (ref. 1) previously conducted using the NASA Ames Research Center's six-degree-of-freedom VMS. A linearized model of a helicopter including rotor flapping dynamics was developed for hover and low-speed flight. Both control and angular-rate cross-coupling were investigated on hingeless and articulated rotor system models. The cross-coupling characteristics were

implemented using physical rotor parameters to maintain realistic combinations of on- and off-axis dynamics. The evaluation tasks consisted of consecutive, timed 100-ft lateral sidesteps and a 30-knot slalom around obstacles. Both tasks were split into two levels of task demands; 10- and 8-sec sidestep timing intervals and two different slalom courses enforced easier and more demanding requirements in each task. The results indicated that task demands and pilot control technique were important in determining allowable levels of coupling; in particular, a degree of cross coupling that is acceptable for one task may be unacceptable for another. In addition, on-axis damping characteristics have a strong effect on the degree of handling qualities deterioration caused by cross coupling. Specific results will be compared with those of the current work in the Results section.

FACILITY DESCRIPTION

The NASA/Army CH-47B variable-stability aircraft provided the in-flight simulation platform for this experiment (fig. 2). It is a large, twin-engine, tandem-rotor helicopter equipped with an explicit-model-following flight-control system (MFCS). An evaluation pilot sits in the right seat and flies the aircraft through the model-following system; a safety pilot on the left monitors the aircraft through the CH-47 basic control system. A brief description of the aircraft flight-control and safety-monitoring systems, summarized from reference 7, follows.

The aircraft has a programmable digital, full-authority, fly-by-wire flight-control system in all four control axes. The evaluation pilot's conventional control arrangement features a longitudinal and lateral cyclic stick with programmable force-feel characteristics, rudder pedals, and collective lever. A digital computer processes the electrical signals generated by these controls and combines them with feedback signals from the on-board sensors, and generates control signals for the parallel full-authority actuators. A DEC PDP 11/73 computer running at a 50-msec frame rate is programmed for flight-control law calculation and data recording. The Electronic Control System (ECS) parallel actuators drive the basic CH-47 control system through rotary clutches which limit the amount of force the actuators can apply through the system.

A hard-over monitoring system is installed to assist the safety pilot in assuring acceptable operation of the ECS actuators. This system causes the rotary clutches to open and the ECS actuators to disengage whenever control rates in the basic CH-47 control system exceed 50% of full throw per second.

EXPERIMENT DESIGN

Since a primary objective of this work was to validate simulation results, the flight experiment was patterned closely on the ground-based simulation experiment. Therefore, the simulation model development and the model characteristics will be described first. Then certain details necessary for implementing the model in the variable-stability aircraft will be identified and discussed. A description of the cross-coupling characteristics and configurations follows. Finally, the flight tasks flown by the pilots for handling qualities evaluation will be described.

Simulation Model Development

The math model used was developed specifically for the ground simulation to model accurately on- and off-axis pitch and roll moments while being as simple as possible. The generic single-main-rotor helicopter model for hover and low-speed flight combined linear aerodynamics with nonlinear kinematics. It included the six body degrees of freedom plus a rotor with second-order longitudinal and lateral flapping dynamics. Rotor coning angle was assumed to be constant during the maneuvers, a reasonable assumption considering the constant altitude tasks involved and the fact that coning is essentially decoupled from flapping in hover. The rotor-flapping and hub-moment equations were linear approximations of those developed by Chen (ref. 8) and used in the ARMCOP (Army Helicopter) (ref. 9) rotorcraft model. These equations model the rotor as a rigid blade and flapping hinge with provisions for a flapping spring and pitch-flap coupling. Lead-lag dynamics were not modeled. Body pitch and roll moments were fully coupled through the rotor-flapping dynamics, as were forward and lateral velocities.

The vertical and directional degrees of freedom were decoupled, and were modeled as first-order responses with damping derivatives chosen for satisfactory (Level 1) handling qualities. Yaw-rate damping combined with directional stability provided good directional response. Similarly, the collective axis included heave-damping and translational-lift effects. Provisions for thrust-yaw coupling due to rotor torque were not included, because the emphasis of this experiment and the tasks involved did not warrant inclusion of this effect.

To consider the influence of on-axis control response and damping on the cross-coupling effects, two basic rotor configurations were examined in addition to the two general types of coupling. An articulated rotor with a flapping-hinge offset of 3.5% was modeled to characterize a helicopter that was satisfactorily responsive in roll and pitch with moderate damping. The hingeless rotor configuration had an effective hinge offset of 15%, giving it very high damping and responsiveness. Both rotor types received satisfactory pilot ratings for the decoupled configurations, so the addition of stability-augmenting control feedback loops was unnecessary.

Implementation of Model in Flight

In adapting the ground-simulation models for in-flight simulation using a model-following control system, the issues of control-system bandwidth and controllable degrees of freedom must be addressed. For acceptable performance, model bandwidth in each axis must be within the capability of the model-following control system. In turn, the achievable bandwidth in the MFCS is limited by the basic inertia and control-moment capabilities of the CH-47, and particularly by the control rates that can be generated without causing system disengagements by the hard-over monitors. In the implementation shown in figure 3, MFCS feed-forwards route the model-attitude accelerations directly to the control commands. Models with high damping and very crisp responses tended to trip the rate monitors frequently. Consequently, it was not possible to implement any of the high-bandwidth, hingeless rotor models that had been used in the ground simulation. In addition, the pitch and roll moments of inertia, I_{xx} and I_{yy}, for the articulated rotor models were increased by 43%. This reduced the pitch and roll moment derivatives to 70% of their simulator values. The model parameters that were used for the flight investigation are listed in table 1.

An additional implementation issue arises from the fact that, in the helicopter, only four degrees of freedom can be controlled using the standard roll, pitch, yaw, and collective controls available.

The longitudinal and lateral velocities are not directly controllable, and the velocity characteristics of the in-flight simulation are those of the basic aircraft. This contrasts with the VMS, where the full six-degree-of-freedom model can be calculated and simulated. If the model is allowed to calculate its own velocities, they will necessarily diverge from those of the aircraft; the model will then generate responses to its own velocities, which are uncorrelated with the actual aircraft states. If the velocity states are removed from the model entirely, it alters the model dynamics to become a rate-command system. The desired model, however, has a lightly damped phugoid, typical of an unaugmented single-rotor helicopter. Therefore, for this experiment, the actual aircraft longitudinal and lateral body-axis velocities, $u_{a/c}$ and $v_{a/c}$, were fed into the model and used in calculating the other states (fig. 3).

The effect of velocity using aircraft velocities on the model-response characteristics can be approximated by substituting CH-47 X and Y stability derivatives (ref. 10) into the model. This is equivalent to an assumption of perfect velocity measurement. For the low frequencies where the velocities have an effect, this is a reasonable assumption. Roll step responses are shown in figure 4 for the model with 1) the original velocity derivatives as used in the VMS simulation, and 2) the aircraft velocity approximation. Use of aircraft velocities in the model appears to have relatively little impact on the model-response characteristics.

In this investigation, the flight-control system was configured for model-following in pitch and roll. "Direct-drive" control of yaw and heave (fig. 3) allowed the pilot inputs to control the basic CH-47 characteristics directly through the ECS actuators. This was consistent with the ground simulation, where vertical and directional responses were chosen simply for good handling qualities and were decoupled. The basic CH-47 with the Stability Augmentation System on is also decoupled with good yaw and heave damping. This minimized the number of sources for potential rate-monitor disengagements.

A secondary issue is the proper calculation of the model kinematics for consistency between the model and aircraft rate and attitude states. The coupled responses in pitch and roll required the full nonlinear kinematic equations for calculating the θ and ϕ attitudes. Therefore, aircraft yaw rate, $r_{a/c}$, is fed into the model and used in the kinematic equations because a corresponding r_{model} is not available (fig. 3). The resulting equations are

$$\dot{\theta}_m = q_m cos\phi_m - r_{a/c} sin\phi_m \tag{1}$$

$$\dot{\phi}_m = p_m + q_m sin\phi_m tan\theta_m + r_{a/c} cos\phi_m tan\theta_m \tag{2}$$

Cross-Coupling Characteristics

The two general types of coupling identified by previous researchers, control and angular-rate, were examined in this investigation as well. Physical rotor parameters in the model were used to implement both types of cross coupling. The purpose of using physical rotor parameters as experimental variables was not to define the coupling limits in terms of them, but rather to maintain realistic combinations of on- and off-axis rotor responses. Pitch-flap coupling (δ_3) and control advance angle (ψ_0) were used to vary the cross-coupling characteristics of the helicopter. The advance angle has the effect of changing the longitudinal- and lateral-cyclic control mixing between the stick and the swashplate without affecting the basic aircraft stability characteristics. Pitch-flap coupling, on the other hand, can significantly change both the on- and off-axis stability characteristics of the helicopter as well as the control effectiveness. Pitch-flap coupling is measured by the

effective flapping-hinge angle relative to the blade (fig. 1) and couples the blade's flapping angle to its pitch angle. It was chosen as an experimental variable, because its primary influence is on the off-axis derivatives L_q and M_p with a relatively minor effect on M_q and L_p. For example, figure 5 illustrates the effects of δ_3 variation from $-30°$ to $+30°$ on the damping and coupling derivatives for the hingeless rotor configuration.

The coupling characteristics are not fully described by the L_q/L_p and M_p/M_q ratios alone. The frequency-domain characterization of the cross-coupling is also a function of the on-axis response in pitch and roll. To illustrate this point, consider the rolling and pitching moment equations

$$\dot{p} = L_p p + L_q q + L_u u + L_v v + L_{\delta a}\delta_a + L_{\delta e}\delta_e \tag{3}$$

$$\dot{q} = M_p p + M_q q + M_u u + M_v v + M_{\delta a}\delta_a + M_{\delta e}\delta_e \tag{4}$$

The velocity terms affect primarily the low-frequency characteristics that are seen by the pilot dynamically as a lightly damped phugoid and statically as cyclic-trim migration with airspeed. For this simplified analysis, therefore, the effects of these terms are considered below the pilot's primary control frequencies, and the terms are not included.

Control coupling can be characterized as a relatively high-frequency effect. For a purely control-coupled configuration ($M_p = L_q = 0$), the resulting moment equations have the following form:

$$\dot{p} = L_p p + L_{\delta a}\delta_a + L_{\delta b}\delta_b \tag{5}$$

$$\dot{q} = M_q q + M_{\delta a}\delta_a + M_{\delta b}\delta_b \tag{6}$$

The roll-to-pitch and pitch-to-roll cross-coupling transfer functions can then be identified as

$$\frac{q}{p}\Big|_{\delta a} = \frac{M_{\delta a}}{L_{\delta a}}\left(\frac{s - L_p}{s - M_q}\right) \tag{7}$$

$$\frac{p}{q}\Big|_{\delta b} = \frac{L_{\delta b}}{M_{\delta b}}\left(\frac{s - M_q}{s - L_p}\right) \tag{8}$$

The frequency-response-magnitude asymptotes are shown in figure 6 for the two control-coupling transfer functions. The lead and lag break-point frequencies are determined by the on-axis damping derivatives M_q and L_p. The magnitude of the low-frequency asymptote is equal to the tangent of the cross-control phase angle and is independent of the damping inherent in the rotor system. At high control frequencies, the pitch-to-roll coupling is greater than the roll-to-pitch because of the difference in fuselage I_{xx} and I_{yy} moments of inertia.

In order to isolate the effects of the control coupling from angular-rate coupling, a value of blade pitch-flap coupling (δ_3) was chosen to eliminate the L_q and M_p stability derivatives. The ideal decoupling δ_3 was $9°$ for the articulated rotor. It should be noted that, for this value of δ_3, the ideal control decoupling ψ_0 was $15°$. The control-coupling configurations are listed in table 2. This is a subset of those evaluated in the ground simulation, differing only by the moments of inertia. Control advance angles from $15°$ to $60°$ yielded cross-control phase angles of $0°$ to $45°$.

In comparison with the frequency-response characteristics of control coupling, angular-rate coupling tends to be a mid-frequency effect. For a purely angular-rate-coupled configuration with no control coupling ($M_{\delta a} = L_{\delta e} = 0$), the simplified moment equations are

$$\dot{p} = L_p p + L_q q + L_{\delta a}\delta_a \tag{9}$$

$$\dot{q} = M_p p + M_q q + M_{\delta e}\delta_e \tag{10}$$

The corresponding roll-to-pitch and pitch-to-roll cross-coupling transfer functions are

$$\frac{q}{p}\Big|_{\delta a} = \frac{M_p}{s - M_q} \tag{11}$$

$$\frac{p}{q}\Big|_{\delta e} = \frac{L_q}{s - L_p} \tag{12}$$

The high-frequency roll-off above $-M_q$ in pitch and $-L_p$ in roll is evident in the magnitude asymptote plots in figure 7. For the same L_q/L_p ratio, it is clear that a rotor system with high damping in pitch and roll has the potential for cross-coupling at a higher frequency than a lightly damped rotor. The actual frequency of the cross-coupled disturbance is dependent on the frequency of the on-axis control task, and may be well within the cross-coupling bandwidth.

Pitch-flap coupling δ_3 angles from $-30°$ to $+30°$ created the range of angular-rate coupling tested in the ground simulation. Each configuration had a corresponding control advance angle calculated to eliminate control-coupling. The angular-rate-coupling configurations evaluated in flight are listed in table 3. This is a subset of configurations tested in the ground simulation. Constraints on available flight time, as compared to the ground simulation, dictated restricting the number of test points as much as possible. Consequently, only δ_3 angles of $-30°$, $-20°$, and $-10°$ were used, yielding L_q/L_p ratios of -1.10, -0.71, and -0.42, respectively.

Evaluation Task

Lateral sidesteps and low-speed slaloms constituted the handling qualities evaluation tasks in the ground simulation. Sidesteps alone were evaluated in flight. As in the ground simulation, two different levels of task demands, enforced by timing intervals, required different levels of aggressiveness in the pilots' control strategy.

The Cooper-Harper Handling Qualities Rating Scale (ref. 11), along with pilot commentary, provided the basis for handling-qualities assessment of each cross-coupling configuration. The scale (fig. 8) balances pilot workload with task performance using a decision-tree structure to assign a single rating, with 1 being the best and 10 being the worst possible scores. The scale can be further broken down into satisfactory, adequate, and inadequate ranges. A critical requirement in applying the Cooper-Harper Scale is to define clearly the desired and adequate task-performance requirements. The specific requirements are summarized below.

The sidestep task consisted of successive lateral translations between position markers spaced 100 ft apart (fig. 9). The markers were orange plastic traffic cones approximately 2 1/2 ft tall, and were lined up in four rows of five cones each. Lining up the row of cones gave precise and consistent lateral position cues. The markers were lined up off the side of a taxiway, the edge of which provided strong longitudinal position cues for the pilot. Height cues were reinforced with a digital radar altimeter readout. A timing signal was used to indicate how quickly each sidestep should be flown. The pilot was asked to stabilize in hover prior to the signal, which simultaneously signaled the start of the next sidestep. A full run included three consecutive steps to the right, then three steps back to the left.

Actual timing intervals from hover to hover were dependent on the particular pilot's ability to achieve desired performance with the decoupled response type. In order to find the critical time interval where pilot ratings began to degrade because of task demands, each pilot flew a series of evaluations with decreasing time intervals. These tests were flown after the pilot had become familiar with the task and the decoupled model. Figure 10 illustrates the effects of time on handling-qualities ratings. Two of the pilots noted no influence of timing on ratings for intervals longer than 10 sec. For these pilots, 10- and 8-sec intervals defined the easier and more difficult tasks. The third pilot's critical timing interval was 11 sec, so his evaluations were made with 11- and 9-sec timing. In addition, one pilot evaluated the moderately rate-coupled model for the interval countdown. It is interesting to note that the "knee" characteristics were similar and occurred at the same timing interval.

Visual position cues available to the pilot were much better in flight than in the simulator because of the increased scene content, ground texture, and field of view. This allowed tighter position limits than in the simulator. Desired performance was defined as achieving a stable hover within $\pm 1/2$ fuselage width (approximately ± 5 ft) laterally, $\pm 1/2$ fuselage length (approximately ± 20 ft) longitudinally, and ± 5 ft vertically. Similarly, for adequate performance, an almost stabilized level hover was expected within approximately twice the position limits just specified. The stable and almost-stable hover requirements were subjective judgments by the pilot.

The evaluation procedure started by first engaging the system in the given model configuration and allowing the pilot a few minutes of flying for familiarization. This usually consisted of performing cyclic-control inputs intended to reveal the general character of the coupling and then practicing a few sidesteps. The pilot then flew a series of sidesteps for evaluation at the longer timing interval. If necessary, a second run was allowed. The ECS system was then disengaged to allow for taking notes and formulating a rating. The shorter interval was evaluated next in a similar manner.

Three pilots participated in the flight evaluations, including one who also participated in the ground-simulation experiment.

MODEL-FOLLOWING PERFORMANCE DOCUMENTATION

Frequency-domain methods were used to determine how well the aircraft responses followed the desired model responses. Three pilot-generated frequency sweeps, each of about 90-sec duration and containing forcing frequencies ranging between 0.3 and 20 rad/sec, were concatenated and analyzed using the techniques described in reference 12. Transfer functions of the same order as the model were then fitted to the data using weighted minimization techniques to determine the poles and zeros of the effective transfer functions and residual equivalent time delays.

The results of the analysis for the decoupled model in the roll axis indicated high-fidelity model-following. Using the model parameters summarized in table 1, including the Y-force derivatives for the CH-47, the desired model transfer function

$$\frac{p_m}{\delta_a} = \frac{s\left[L_{\delta a}s + (L_v Y_{\delta a} - Y_v L_{\delta a})\right]}{s^3 + (-Y_v - L_p)\,s^2 + (L_p Y_v - L_v Y_p)\,s + gL_v} \tag{13}$$

$$= \frac{39.4\,s\,(s + 0.12)}{(s + 3.05)\,(s + 0.022 + 0.49i)\,(s + 0.022 - 0.49i)} \tag{14}$$

was used to plot the frequency response seen in figure 11. Note the low-frequency gain and phase response characteristic of an unaugmented helicopter, which is largely due to the velocity term, L_v, in the rolling-moment equation.

The results of the frequency-sweep analysis are plotted over the range from 0.7 to 9 rad/sec, the range for which there existed good input/output coherence in the flight test data. The 0.078-sec effective time delay associated with the 3-pole, 5-Hz Bessel anti-aliasing filters used to smooth the roll- and pitch-rate gyro signals has been taken into account in the analysis of these data. Finally, a transfer function of the same order as the model was fitted to the flight data over the same frequency range, including a time delay to represent unmodeled higher-frequency effects (fig. 12). The resulting transfer function was

$$\frac{p_{a/c}}{\delta_a} = \frac{16.8s(s+0.36)\,e^{-0.20s}}{(s+2.70)(s+0.012+0.53i)(s+0.012-0.53i)} \tag{15}$$

It can be seen that the roll-rate dynamics of the desired model are reproduced accurately in flight.

Analysis of the model-following in the pitch axis produced similar results. The desired model frequency response is shown in figure 13. The transfer function for the uncoupled model has the same form as in the roll axis, except that the low-frequency complex roots are slightly unstable in pitch. The stability of these phugoid roots is very sensitive to the values of M_u in pitch and L_v in roll.

$$\frac{q_m}{\delta_e} = \frac{s[M_{\delta e}s + (M_u X_{\delta e} - X_u M_{\delta e})]}{s^3 + (-X_u - M_q)s^2 + (M_q X_u - M_u X_q)s + gM_u} \tag{16}$$

$$= \frac{16.8s(s+0.006)}{(s+1.27)(s-0.08+0.45i)(s-0.08-0.45i)} \tag{17}$$

Figure 14 shows the aircraft frequency-response characteristics for this configuration together with the identified transfer function

$$\frac{q_{a/c}}{\delta_e} = \frac{14.6s(s-0.081)\,e^{-0.20s}}{(s+1.17)(s-0.13+0.40i)(s-0.13-0.40i)} \tag{18}$$

The 200-msec time delay in pitch was set to match the roll-axis delay.

The θ/δ_e and ϕ/δ_a attitude-response bandwidths for the decoupled model were measured from the flight data. The phase ($-135°$) and gain (+6 dB) bandwidths measured from the flight data for both the pitch and roll axes are shown below.

Axis	$\omega_{BW,phase}$ rad/sec	$\omega_{BW,gain}$ rad/sec
roll	0.85	2.2
pitch	(see text)	1.4

The unaugmented helicopter model is essentially a rate-command system with low-frequency dynamics induced by the L_v and M_u derivatives. These velocity modes introduce low-frequency phase effects that reduce the phase margins to considerably less than would be expected for a true rate-command system with the same rate damping. In fact, the pitch axis does not even have a phase

bandwidth by definition because the unstable pair of roots at 0.42 rad/sec prevent the phase from ever reaching $-135°$, or, equivalently, $-45°$ in q/δ_e (fig. 14). The phase lags due to the 200-msec time delay are relatively minor: $-11.5°$ at 1 rad/sec. Despite these low bandwidth measurements, however, the pilot handling qualities ratings presented in the Flight Test Results section provide evidence of Level 1 handling qualities for the baseline decoupled model.

In summary, the model-following fidelity proved to be very good in both the pitch and roll axes. Although frequency sweep tests were not conducted for the coupled models, it can be assumed with some confidence that the vehicle dynamics flown by the pilots were those of the desired models with the addition of a 200-msec time delay.

FLIGHT TEST RESULTS

Results of the piloted evaluation of the pitch-roll cross-coupling configurations are presented in the form of control utilization and performance achieved, and pilot opinion. Representative control and performance data are included as time histories, crossplots, and selected spectral analyses. Handling-qualities ratings are based on the standard technique outlined in reference 11 and are complemented by pilot commentary.

It is the objective to illustrate first the basic characteristics of the uncoupled and coupled configurations in order to provide a basis for interpreting the pilot opinion data.

Basic Task Characteristics (Uncoupled Model)

The essential character of the lateral sidestep task is shown in figure 15. The time history data are for a typical run with an uncoupled model consisting of three 10-sec segments to the right, followed by three to the left. Each task segment consists of three distinct phases; (1) an initial roll to establish a bank angle and a lateral acceleration, (2) a short period of steady lateral translation, and (3) a deceleration and stabilization phase. For the entire maneuver, each response variable reflects its own characteristic "task signature." The outer-loop variables (e.g., velocity) exhibit a dominant low frequency with a period close to the 10-sec task interval. However, this signature becomes progressively less unique for the inner-loop variables (e.g., angular rate). Most significantly, the lateral-control time history (fig. 15) contains numerous reversals that require close inspection in order to relate them to the task segments and the phases of each segment.

The time history data shown in figure 15 were used to generate the crossplots of pitch-roll control and response parameters that are shown in figure 16. This presentation of the data provides good visualization of the amount of activity occurring in the longitudinal axis during execution of the lateral task. For the uncoupled configuration, very little longitudinal activity is evident.

Characteristics of the Coupled Configurations

Sample time histories and crossplots are given for the two maximum coupling configurations. Figures 17 and 18 are taken from flight data for the model having 45° of control coupling. Figures 19 and 20 correspond to the model having a response coupling ratio $|L_q/L_p| = 1.10$. For both

of these configurations, there is considerable activity in the longitudinal axis, although performance errors as measured by longitudinal velocity (and corresponding position error) were kept small. The time history plots indicate that oscillatory characteristics are associated with both configurations. The crossplot presentations reveal that the control activity is characterized for the control-coupled model by sweeping circular motions (fig. 18), suggesting a dominant phase difference between the two signals, whereas the response-coupled model (fig. 20) seems not to be characterized by any correlated activity. With an important exception to be noted subsequently, the crossplotted control and response data for all pilots and all runs appeared remarkably similar in these respects.

Spectral analysis of the data was performed to further analyze the pilot's control utilization associated with the coupled configurations. For the case of 45° control coupling, autospectrums for roll and pitch control inputs are presented in figure 21. Close inspection of the time history data indicates that the spectral peaks occurring near 0.6 rad/sec, 1.2 rad/sec, and 1.9 rad/sec in both controls are associated with the basic task interval, the initial roll-in phase, and the stabilization phases, respectively.

To further investigate the relationship between the pilot's use of the roll and pitch controls, the cross correlation and the transfer function were also calculated. The results are shown in figure 22. The pitch control inputs are seen to lag the roll inputs by about 45° at the roll-in frequency, and by about 90° at the stabilization frequency. The same characteristic peaks in the control autospectra also existed for the response-coupled case. However, no comparable linear correlation between the two controls was apparent. Similarly, no correlation between roll- and pitch-control activity was apparent from spectral analyses of the uncoupled case, a situation already evidenced in the crossplot data of figure 20.

Analysis of the test data in the frequency domain in this way serves to quantify the basic characterization of the the pilot's control usage beyond what can be observed in the time history and the crossplot presentations. In addition, it will be shown that the differences in control character between the two types of coupling correlate with the pilot-opinion data.

Pilot Opinion Data

Pilot opinion results are presented in the form of Cooper-Harper pilot ratings (ref. 11) and pilot commentary. Pilot ratings are presented separately for control and angular-rate response coupling, with pilot comments used to describe the characteristics of each. In addition, the ratings are compared with those obtained in the VMS ground simulation.

Angular-rate coupling– The pilot ratings for the angular-rate-coupling configurations are presented in figure 23. A total of 48 pilot evaluations from three pilots contributed to the data. The following paragraphs discuss important features of the data and make comparisons with the simulation results.

The more difficult demands of the shorter time interval task are evident from the data (fig. 23), which show a consistent one to one-and-a-half pilot rating degradation from the longer time interval for all angular-rate-coupling configurations. This contrasts with the data from the ground simulation (ref. 1) where pilot techniques for the same tasks varied widely in aggressiveness as measured by the peak roll rates achieved during the task. This aggressiveness, and the resulting pilot ratings, were uncorrelated with the ostensible task demands imposed by the timing interval, despite the stated task being to fly the sidesteps as smoothly as possible while meeting the performance criteria.

For this reason, subsequent reference to the *simulation* sidestep results will combine both the 8- and 10-sec ratings into one average. The comparison between in-flight and simulation results could indicate that the full-fidelity motion and visual-cue environment available in flight induced a more consistent pilot technique than in simulation. In the CH-47, however, aggressiveness levels were also constrained artificially in order to preclude disengagements of the variable-stability system by the control-rate monitors. Primarily, this served to limit the rapidity with which the initial roll angle could be established. Two pilots commented on being so constrained, although the third pilot, in the entire process of learning the task and performing the evaluations, scarcely encountered the trip limits. These factors suggest that the combination of full-fidelity cueing and control-rate restrictions contributed to more consistent task-related handling qualities results in flight, although it is not clear which is predominant.

Figure 24 compares the pilot ratings from simulation and flight. The simulation ratings are the averages of both 8- and 10-sec interval evaluations for the reasons discussed previously. In order to be most compatible, only the flight test ratings from the shorter intervals are compared, although the trends for either or their average are the same. At low levels of $| M_p/M_q |$ coupling, the handling qualities ratings from flight are slightly worse than in simulation, although all the ratings have similar slopes. At high levels of $| M_p/M_q |$, the rate of deterioration in handling qualities is less for the flight configurations than for the simulation models. The on-axis damping characteristics were shown in the ground simulation to influence the severity of the angular-rate coupling (ref. 1). At high levels of $| M_p/M_q |$, the moderately damped articulated-rotor models demonstrated less deterioration in handling qualities than did the highly damped hingeless rotor models. This conclusion was consistent with the frequency-dependent character of the angular-rate coupling; the roll-rate-to-pitch-rate coupling, $q/p\,|_{\delta a}$, was shown in figure 7 to approximate a first-order lag with high-frequency magnitude roll-off above the pitch damping frequency, $-M_q$. Less damping yields a lower-frequency breakpoint for the coupling, and therefore lower cross-coupling bandwidth potential. Although the data are not clear-cut, the flight results tend to corroborate this damping dependency established in the simulation.

Pilot comments for these angular-rate-coupled configurations describe the off-axis response characteristics as unpredictable compared to the control-coupled configurations. This made it difficult to develop an effective decoupling crossfeed technique, and, instead, the pitch disturbances were compensated for as they developed. This supports the previous observations based on the crossplot presentations (fig. 20) and the spectral analyses of the task data.

Control coupling– Figure 25 shows the pilot ratings for the control-coupling configurations evaluated in flight. The data are based on 43 pilot evaluations and ratings, including those for the decoupled baseline configuration. Several important points are made in the following paragraphs about the flight data by itself and in comparison with simulation results.

Similar to the response-coupled configurations, there is a consistent degradation in the pilot ratings for the shorter time interval task. This is also in disagreement with the simulation results for these configurations.

With two notable exceptions, the difference in the pilot ratings at each test condition is relatively small. This would indicate a relatively consistent pilot technique in terms of both aggressiveness and learning effects. The stray rating points in figure 25 marked by *A* and *B* require examination, however. In the case of *A*, the rating of 7 follows a rating of 4 for the longer interval with the same coupling. The pilot's comments suggested that learning effects may have been a factor. For the longer interval, he noted that he was able to use a "lower gain on arrestment [of velocity] to minimize off-axis response." For the more difficult shorter-time task, he noted that an "increase

in pilot gains resulted in a larger, less predictable off-axis response." After the flight, he indicated that his initial pitch-control inputs seemed to be in the wrong direction and may have been making the coupling worse. The coupling characteristics of the configuration immediately preceding were in the opposite direction, supporting the hypothesis that a crossfeed just learned for the first configuration had adversely carried over to the second. The first configuration, a moderate rate-coupled model ($|L_q/L_p| = 0.71$), had been flown extensively during evaluations of a time interval countdown from 11 to 7 sec for the purposes discussed in the Evaluation Tasks section. The direction of the coupling for the two cases was opposite: from roll-right/pitch-up to roll-right/pitch-down. Because of these factors, which question the validity of this data point, it is not included in the averaging. A restriction in available flight time precluded a repeat of this test point. Nonetheless, this situation seems to indicate that significant learning effects are involved in adapting to significantly different configurations.

Similar learning effects explain the rating of 4 for the longer time interval task associated with point *B* in figure 25. This test point immediately followed evaluation of the 30° control-coupling case for longer and shorter intervals with ratings of 5 and 7, respectively. When next evaluating the 45° coupling case for the longer task, the pilot apparently found it significantly easier to accomplish, and commented on his capability to "lead with the control correction for the cross-coupled response in the pitch axis." Under these circumstances, the coupling was described as "annoying." However, for the tighter, more aggressive control required for the shorter task, it was "hard to determine how large an input was needed to correct the cross-coupled error, involving a high mental workload." The rating given was 7, consistent with the other evaluations of that configuration.

The significantly better rating for the longer task, and the reason for it, is supported by the crossplot of the pilot's control utilization shown in figure 26. A coupled control character involving no apparent phase lag between the roll and the pitch inputs is apparent, and is in significant contrast to the crossplot data shown earlier for the same configuration and another pilot in figure 18.

Two cases have been presented where significant learning effects have yielded significantly different, but legitimate, results. These examples reinforce the need to consider these factors when drawing conclusions about acceptable or unacceptable levels of cross-coupling. In particular, the effects of system failures or other circumstances that might suddenly present the pilot with a large change in coupling characteristics must be considered.

Direct comparison of the pilot ratings between simulator and flight shows a negligible difference (fig. 27). The simulator data are from the highly damped hingeless rotor models only. The flight-generated ratings are for the shorter-interval task. These data alone would suggest that the on-axis damping characteristics are not an issue for control coupling. This conclusion, however, contrasts dramatically with the simulator results for the slalom task. In that task, the coupling-induced deterioration in handling qualities was significantly greater for the less-damped models. It is difficult to compare these different results, however, because of the number of variables involved: slalom versus sidestep task, simulator versus in-flight, and consistent versus inconsistent pilot technique and aggressiveness.

All pilots commented on the ability to generate conscious cyclic-control crossfeeds after some learning, particularly during the initial roll-in phase of the sidestep. Roll control during this phase is predominantly open-loop, and it is relatively easy to learn the crossfeed required to suppress most of the associated pitch response. One pilot evaluated the 45° coupling case for the longer-interval task and experienced considerable pitch and roll oscillations during all phases of the sidesteps. He was not aware of any crossfeeds in his control strategy and gave a pilot rating of 7. On the subsequent short-interval evaluation of the same coupling, he commented that he "learned during

these runs how to do the inputs so it wasn't as bad as I had expected" from the longer runs and that he now saw "no problems with coupling when starting the sideward flight, but severe coupling was felt when arresting the aircraft velocity." His rating was the same (7), indicating that the crossfeed strategy allowed improved time performance without increased workload. Another pilot noted that he "used crossfeeds, but wasn't real confident [that he] knew exactly how to crossfeed except on roll-in and roll-out." This led him to state "the need to plan the maneuver to compensate for the control shortcomings: a fast as possible entry roll-in [to allow maximum time for a] smooth as possible roll-out." Supporting evidence for effective pilot crossfeeds is given by the 45° phase lags identified for the roll-in frequencies from the spectral analysis discussed in the previous section.

The higher gains required during the stabilization phase apparently made conscious crossfeeds ineffective. Perhaps more training time for the pilots would change that. All pilots experienced consistent oscillations in pitch and roll during the stabilization to hover; the 45° coupling configuration in particular was noted as having "lots of PIO [pilot induced oscillation] potential in both axes together." The tendency was for the pilot to chase the pitch and roll around in a circle, with each control correction causing a disturbance in the next axis. One pilot in the ground simulation referred to this condition as "hubcapping" (ref. 1). Recall, from figure 21, that the identified dominant frequencies of 1.2 and 1.9 rad/sec corresponded to the roll-in and stabilization phases of the task, respectively. In addition, the control-coupling frequency-response characteristics show that the increase in frequency causes the coupling magnitude to increase in pitch-to-roll while decreasing in roll-to-pitch. Higher-bandwidth pilot control in pitch then couples strongly into roll, leading to increased sensitivity to "hubcapping." The spectral analysis data in figure 22 and the crossplot presentations in figure 18 corroborate this situation by identifying a 90° phase lag between axes at the stabilization-phase frequency.

CONCLUSIONS

A piloted in-flight simulation experiment was conducted on the NASA/Army CH-47B variable stability helicopter to assess the effects on handling qualities of varying types and degrees of pitch-roll cross coupling in helicopters during near-terrain flight. This work was an extension of a piloted ground simulation conducted on the NASA Ames Research Center VMS, and was intended to validate the simulation results. Two basic types of coupling, control and angular-rate, were evaluated on a model of an unaugmented helicopter. Good quality reproduction of the simulation model characteristics was achieved in the in-flight implementation. The on-axis pitch and roll damping was reduced from simulator levels for compatibility with the aircraft flight-control system; this change yielded new data which validated and extended the simulation results.

Based upon the pilot evaluation and flight data from this experiment, the following conclusions are drawn.

1. Both ground and in-flight simulation experiments demonstrated that degradations in handling qualities occur with increased levels of cross-coupling, regardless of its type.

2. On-axis damping characteristics determine the impact of cross-coupling on handling qualities. The flight results support simulator-based conclusions that increased damping causes increased sensitivity to the angular-rate coupling metric $|L_q/L_p|$. For the level of L_p in the flight experiment (-2.7), no angular-rate coupling level was rated in the inadequate category.

3. In comparison with the ground simulation, the pilot control techniques demonstrated in flight were generally more consistent in terms of aggressiveness and handling qualities ratings.

The combination of full-fidelity motion/visual cueing and the control input rate restrictions in flight contributed to this result.

4. Flight and ground-based data both indicate a maximum of approximately 30° control coupling for adequate handling qualities. This boundary, however, is strongly dependent on the demands of the task.

5. Pilot learning has a significant impact on performance and workload. Sudden changes in coupling characteristics required some practice. Control strategies learned for a given coupling tended to carry over into the next. This is an important result. Although modern stability and control augmentation system (SCAS) designs may be able to decouple any aircraft, a SCAS failure causing sudden reversion to highly coupled characteristics in nap-of-the-Earth flight could be difficult for the pilot to control.

REFERENCES

1. Watson, Douglas C.; and Aiken, Edwin W.: An Investigation of the Effects of Pitch-Roll Cross Coupling on Helicopter Handling Qualities for Terrain Flight, AIAA Paper 87-2534, Aug. 1987.

2. Garren, John F., Jr.: Effects of Coupling Between Pitch and Roll Control Inputs on the Handling Qualities of VTOL Aircraft, NASA TN D-1233, 1962.

3. Chen, Robert T. N.; and Talbot, Peter D.: An Exploratory Investigation of the Effects of Large Variations in Rotor System Dynamics Design Parameters on Helicopter Handling Characteristics in Nap-of-the-Earth Flight, Proc. 33rd Ann. National Forum Amer. Helicopter Soc., Washington, D.C., May 1977.

4. Corliss, Lloyd D.; and Carico, Dean G.: A Flight Investigation of Roll-Control Sensitivity, Damping, and Cross-Coupling in a Low Altitude Lateral Maneuvering Task, NASA TM-84376, 1983.

5. White, Fred; and Blake, Bruce B.: Improved Method of Predicting Helicopter Response and Gust Sensitivity, Proc. 35th Ann. National Forum Amer. Helicopter Soc., Washington, D.C., May 1979.

6. Chen, Robert T.N.: Selection of Some Rotor Parameters to Reduce Pitch-Roll Coupling of Helicopter Flight Dynamics, National Specialists' Meeting on Rotor System Design, Amer. Helicopter Soc., Mideast Reg., October 1980.

7. Hilbert, Katherine B.; Lebacqz, J. Victor; and Hindson, William S.: Flight Investigation of a Multivariable Model-Following Control System for Rotorcraft, AIAA Paper 86-9779, April 1986.

8. Chen, Robert T.N.: A Simplified Rotor System Mathematical Model for Piloted Flight Dynamics Simulation, NASA TM-78575, 1979.

9. Talbot, Peter D.; Tinling, Bruce E.; Decker, William A.; and Chen, Robert T.N.: A Mathematical Model of a Single Main Rotor Helicopter for Piloted Simulation, NASA TM-84281, 1982.

10. Weber, Jeanine M.; Liu, Tung Y.; and Chung, William: A Mathematical Simulation Model of a CH-47B Helicopter, NASA TM-84351, 1984.

11. Cooper, George E.; and Harper, Robert P.: The Use of Pilot Rating in the Evaluation of Aircraft Handling Qualities, NASA TN D-5153, 1969.

12. Tischler, Mark B.: Frequency-Response Identification of XV-15 Tilt-Rotor Aircraft Dynamics, NASA TM-89428, 1987.

$\gamma = 4.9$ Lock No.	$\omega = 483$ rpm	$I_{xx} = 329$ slug$-$ft^2
$\epsilon = 3.5\%$ hinge offset	b = 4 blades	$I_{yy} = 899$ slug$-$ft^2
R = 13.2 ft	W = 2550 lbs	$h_r = 2.8$ ft rotor height

Table 1: Basic model parameters.

cross-control phase angle	$L_{\delta a}/L_p$ (deg/s/in)	$M_{\delta e}/M_q$ (deg/s/in)	$L_{\delta e}/L_p$ (deg/s/in)	$M_{\delta a}/M_q$ (deg/s/in)	$\frac{L_{\delta e}M_q}{M_{\delta e}L_p}$	$\frac{L_{\delta e}}{M_{\delta e}}$	$\frac{M_{\delta a}}{L_{\delta a}}$
0°	−8.0	−13.3	−0.1	0.1	0.01	0.03	0.00
15°	−8.0	−13.3	−5.1	3.0	0.28	0.76	0.10
30°	−8.0	−13.3	−9.6	5.8	0.59	1.61	0.22
45°	−8.0	−13.3	−13.5	8.1	1.02	2.78	0.37

Table 2: Control-coupling model characteristics.

δ_3	$\dot{\psi}_0$	L_p (1/sec)	L_q (1/sec)	M_q (1/sec)	M_p (1/sec)	$L_{\delta a}/L_p$ (deg/s/in)	$M_{\delta e}/M_q$ (deg/s/in)	$\lvert M_p/M_q \rvert = \lvert L_q/L_p \rvert$
9°	15.0°	−3.0	0.0	−1.1	0.0	8.0	13.3	0.0
−10°	−4.6°	−3.1	−1.3	−1.1	0.5	8.0	13.3	0.42
−20°	−15.5°	−2.8	−2.0	−1.0	0.7	8.0	13.3	0.71
−30°	−26.6°	−2.3	−2.5	−0.8	0.9	8.0	13.3	1.10

Table 3: Angular-rate-coupling model characteristics.

ORIGINAL PAGE IS
OF POOR QUALITY

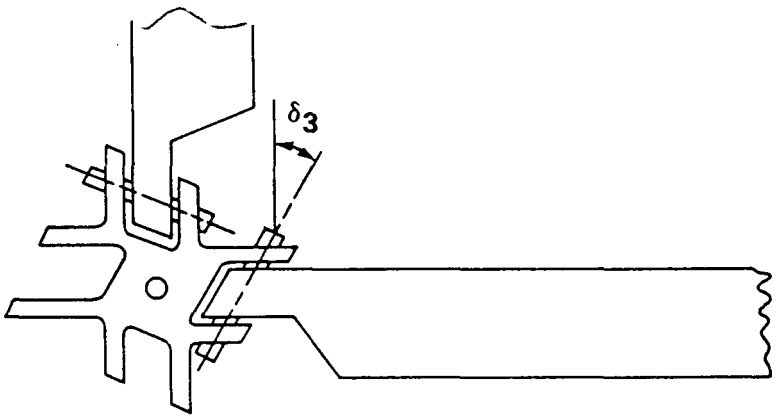

Figure 1 - Pitch-flap coupling, δ_3.

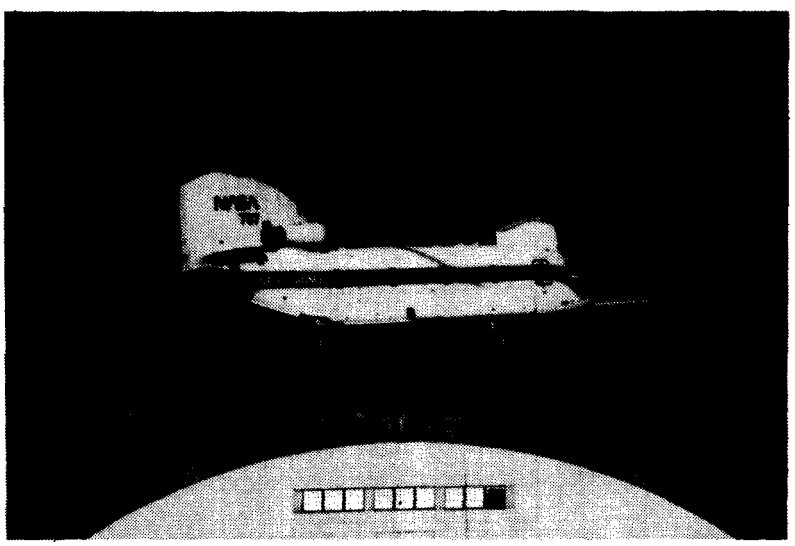

Figure 2 - NASA/Army CH-47B Variable Stability Helicopter.

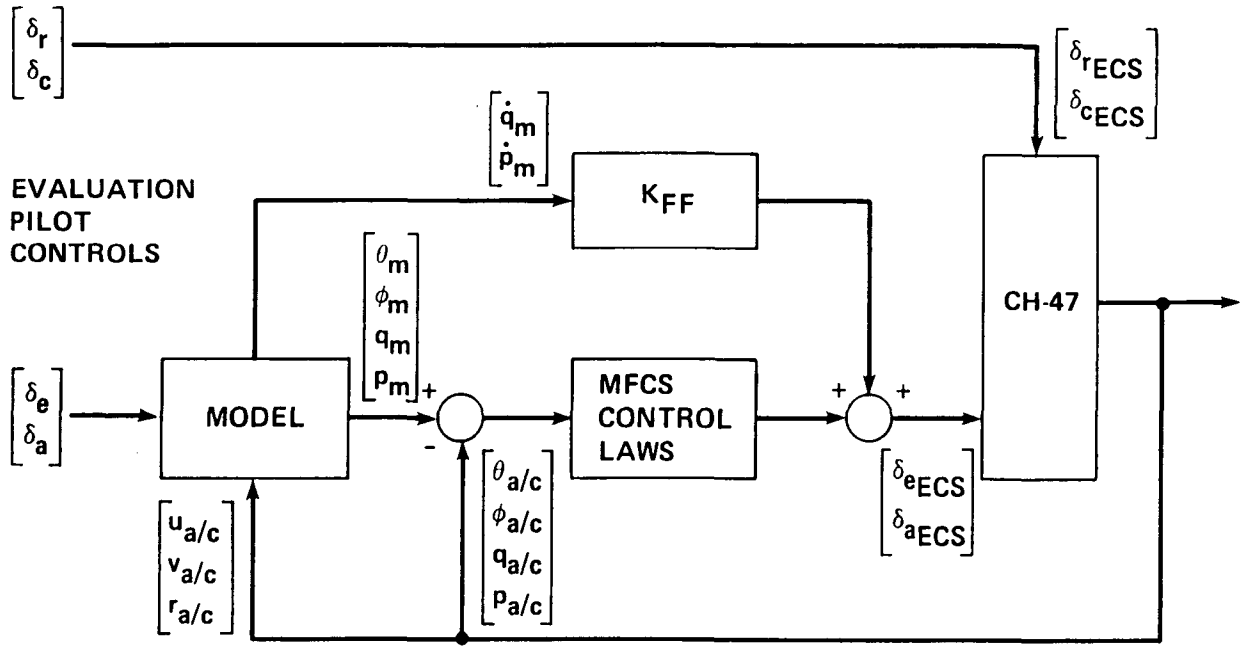

Figure 3 - Model-following control system implementation.

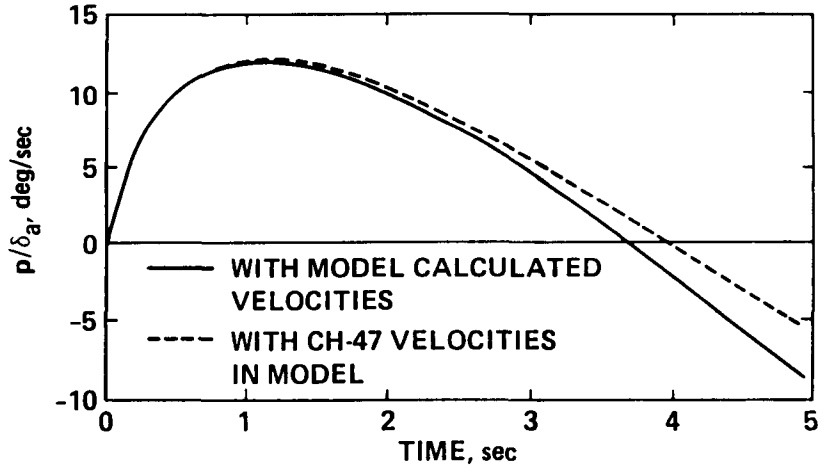

Figure 4 - Comparison of roll responses to step lateral control input, decoupled model (a) with simulation velocity derivatives, and (b) with CH-47 u_b and v_b velocity approximation.

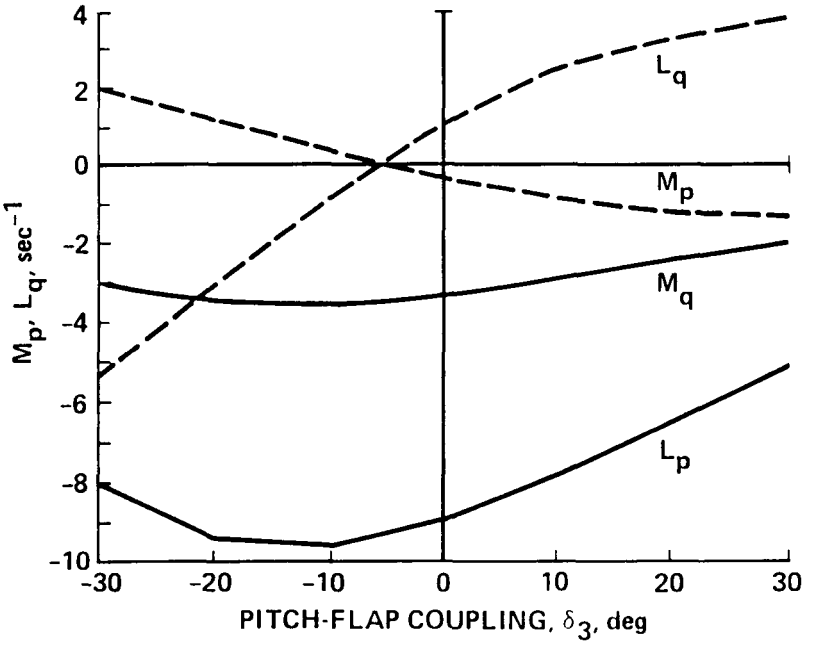

Figure 5 - Damping and coupling derivatives versus pitch-flap coupling angle for the hingeless rotor.

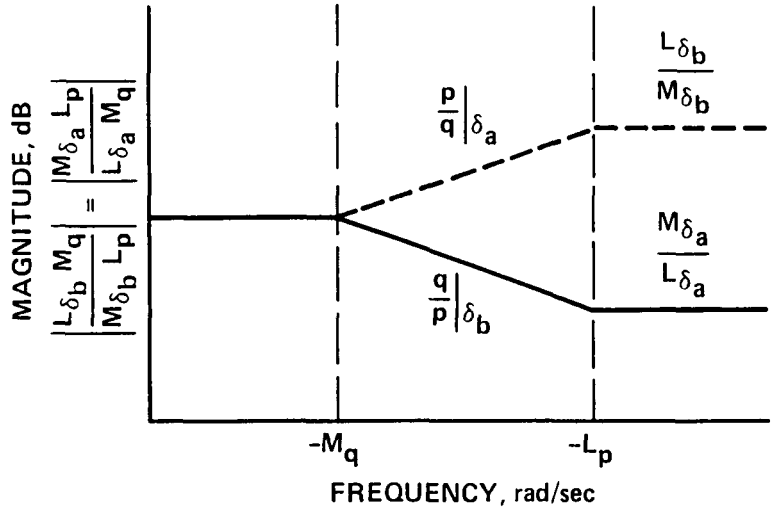

Figure 6 - Control-coupling frequency-response asymptotes for simplified two-degree-of-freedom model.

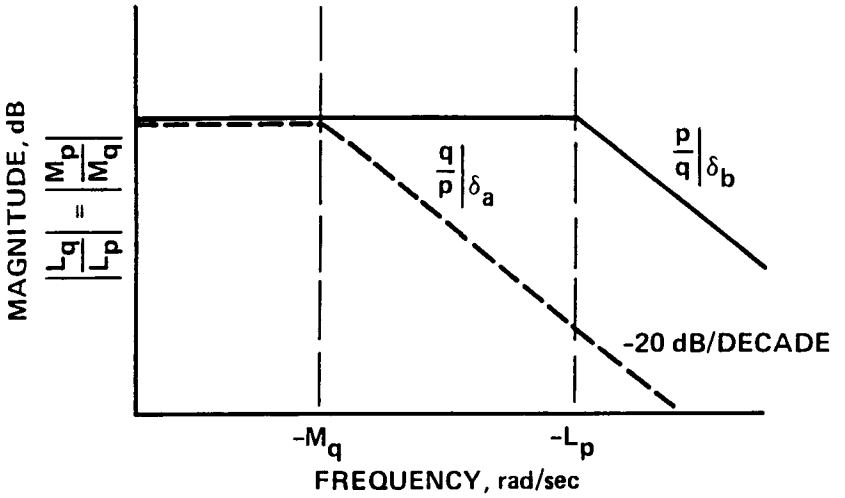

Figure 7 - Angular-rate-coupling frequency-response asymptotes for simplified two-degree-of-freedom model.

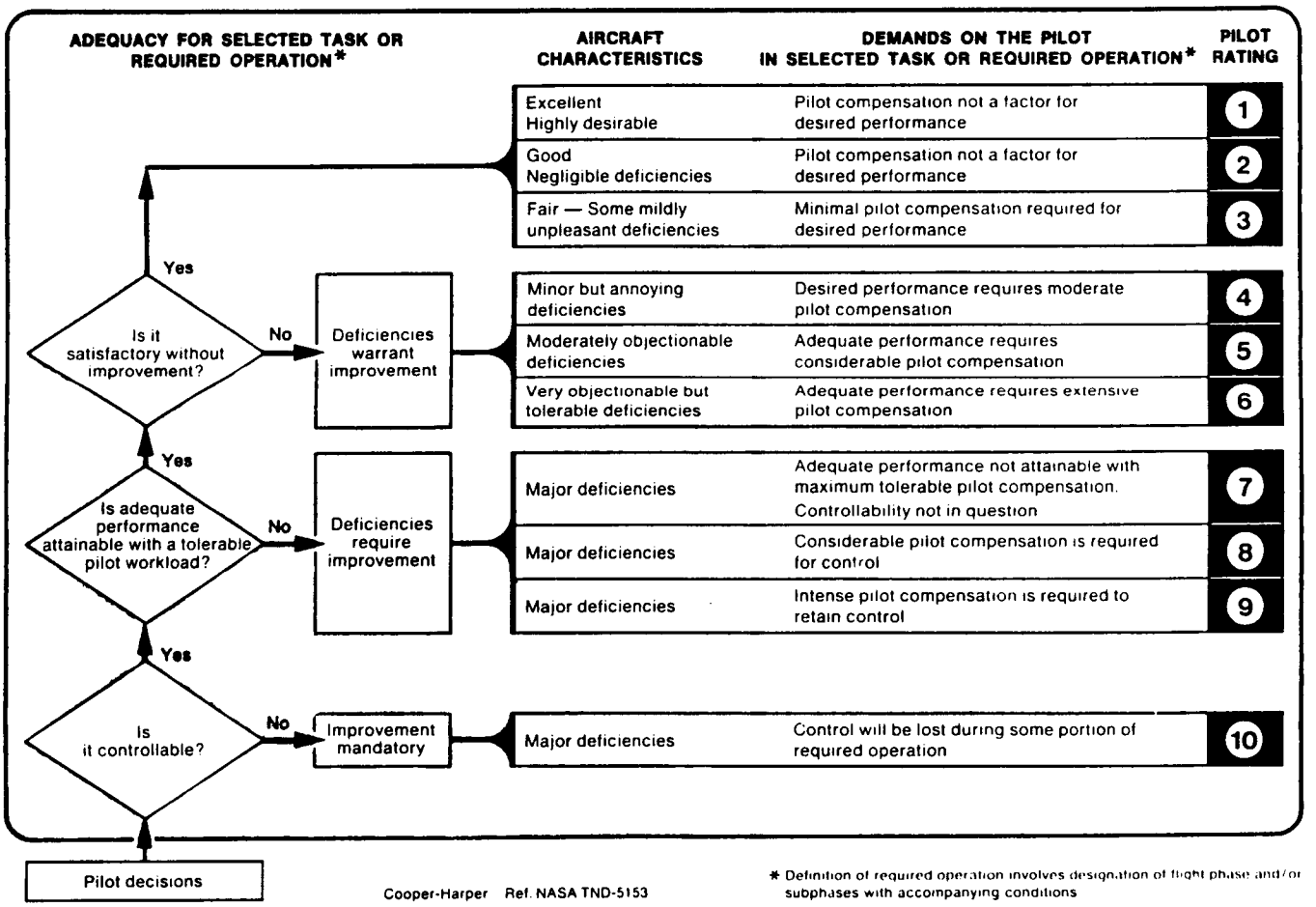

Figure 8 - Cooper-Harper handling-qualities rating scale.

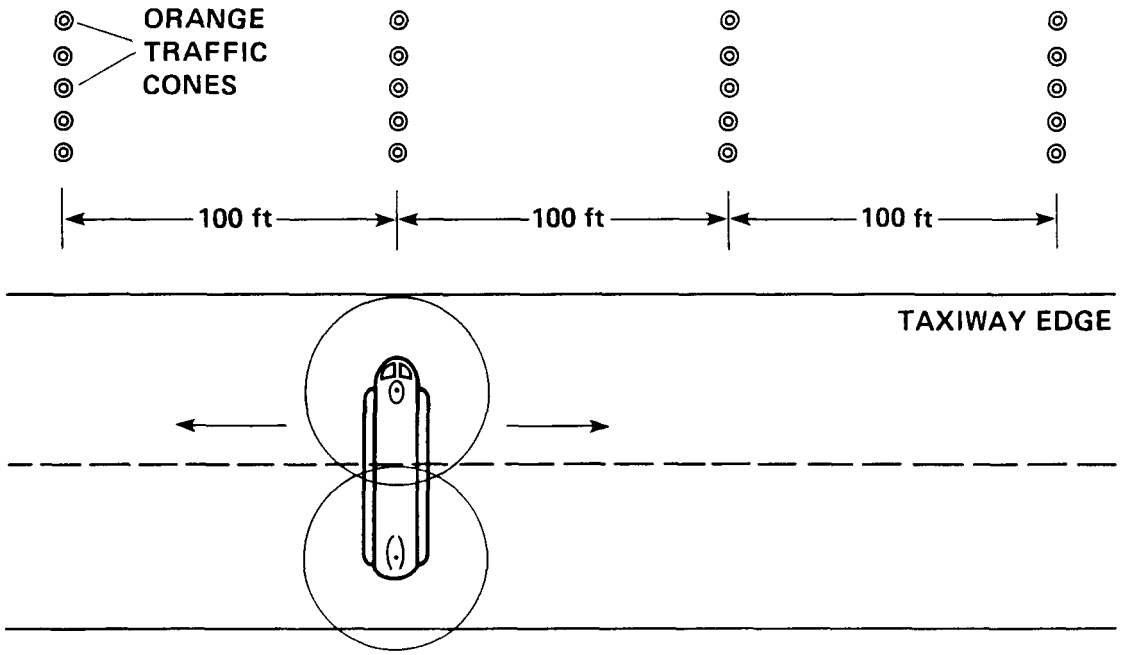

Figure 9 - The 100-ft lateral sidestep course: three right, three left.

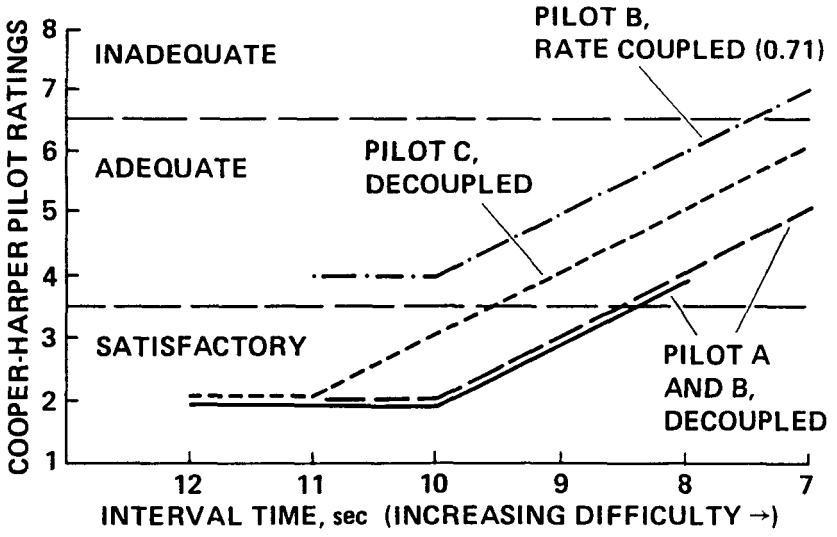

Figure 10 - Pilot ratings versus decreasing time intervals in the sidestep task.

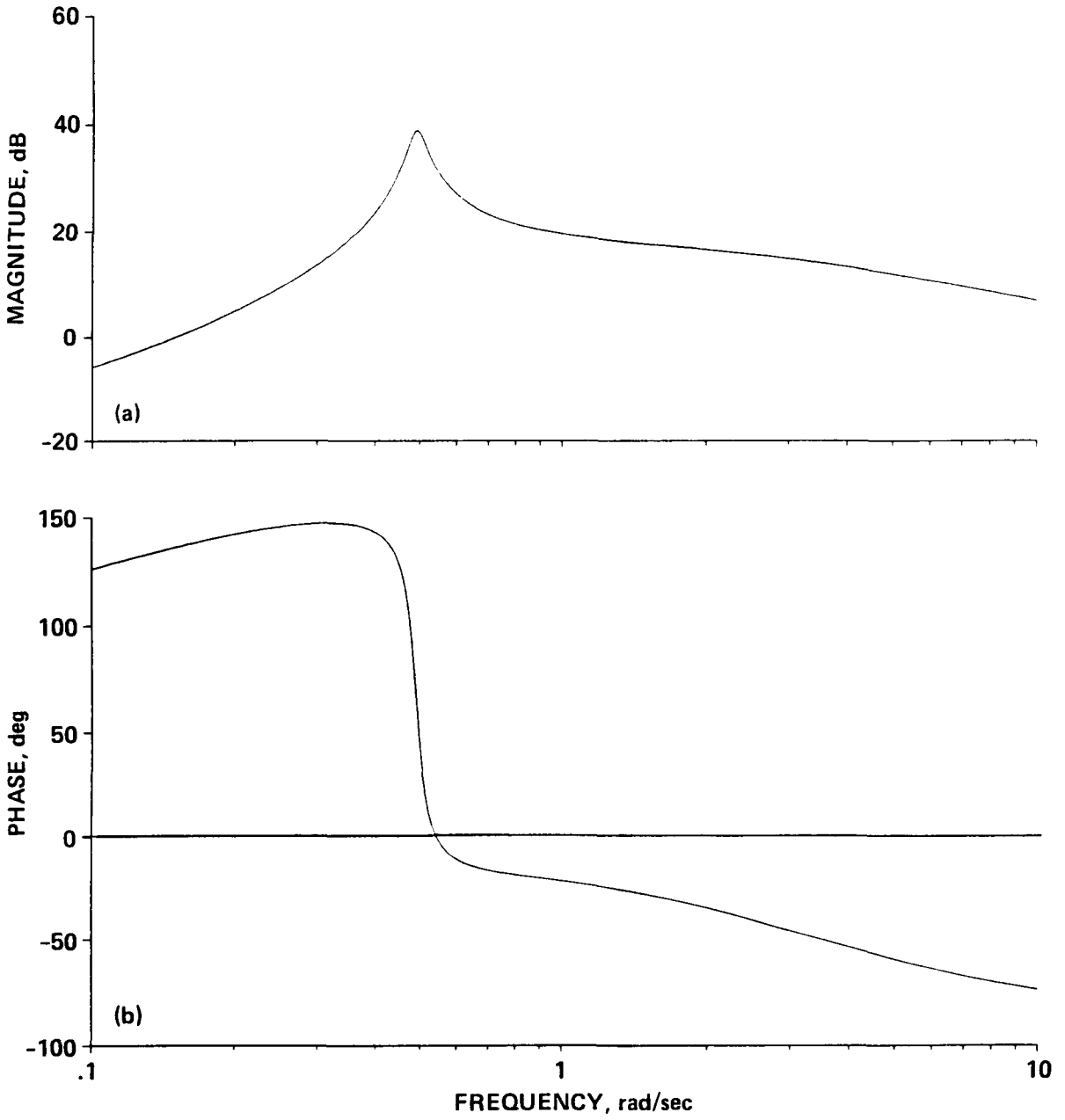

Figure 11 - p/δ_a frequency response for the decoupled model.

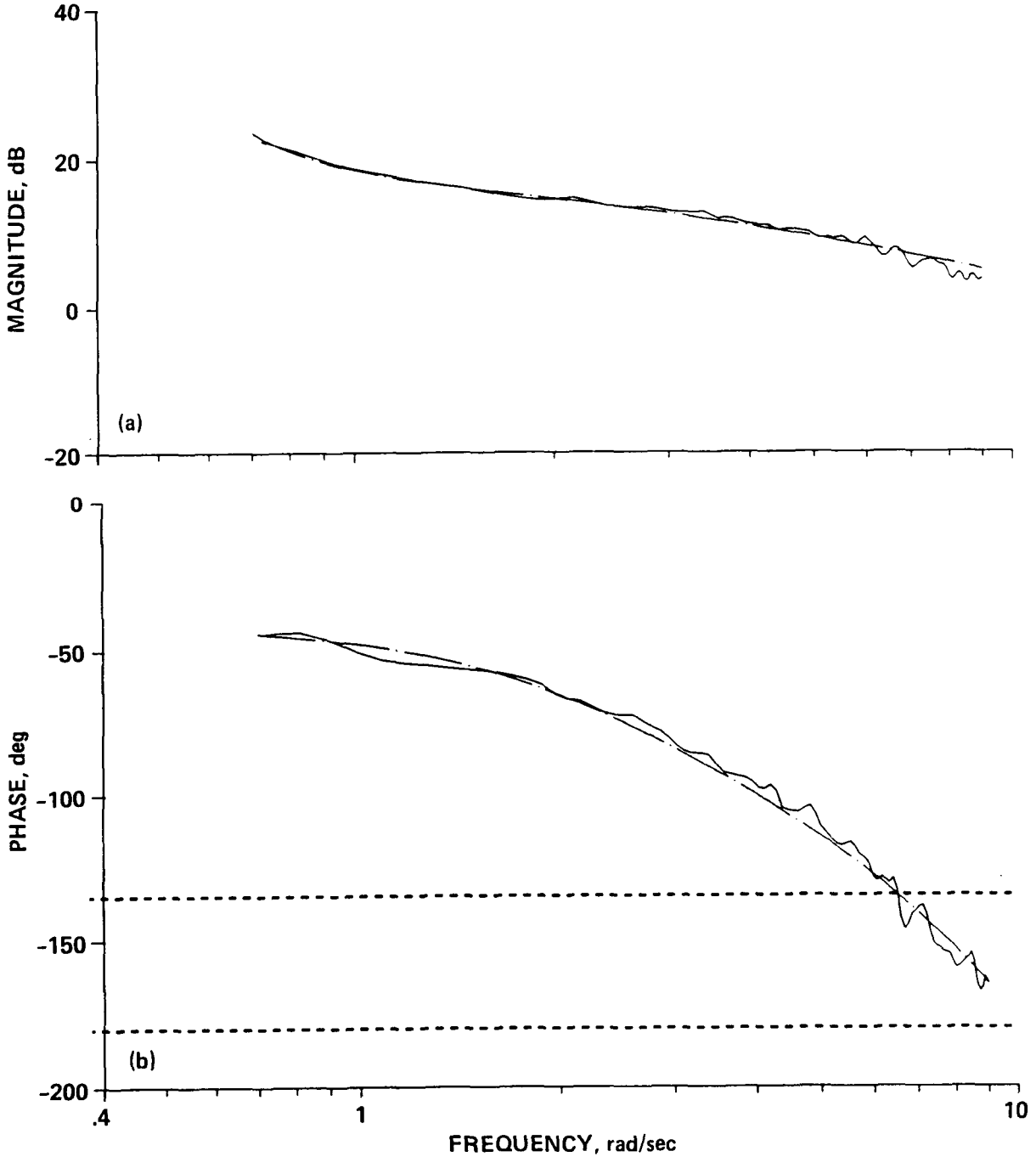

Figure 12 - p/δ_a frequency response for the decoupled configuration, flight data and fitted transfer function.

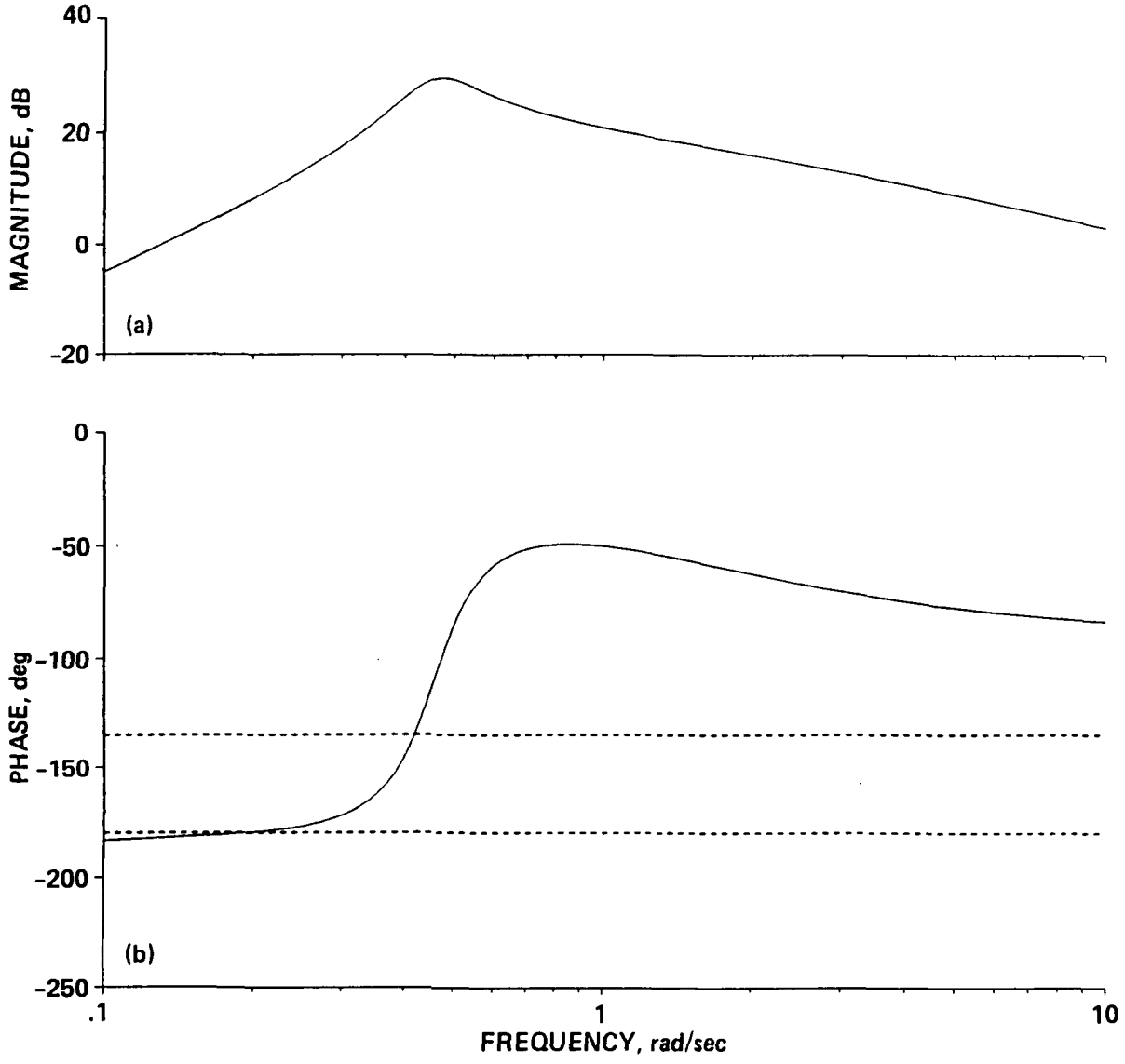

Figure 13 - q/δ_e frequency response for the decoupled model.

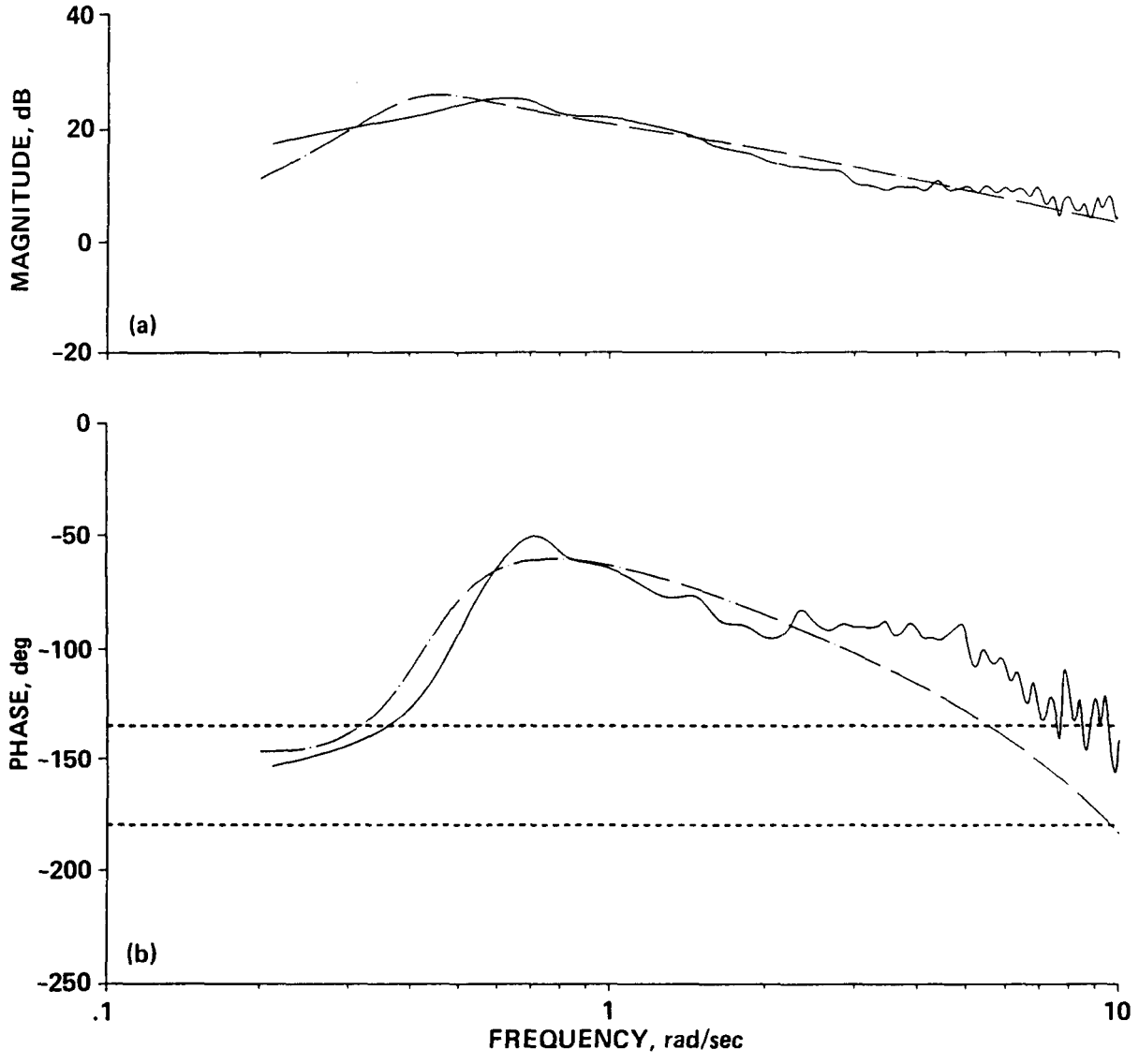

Figure 14 - q/δ_e frequency response for the decoupled configuration, flight data and fitted transfer function.

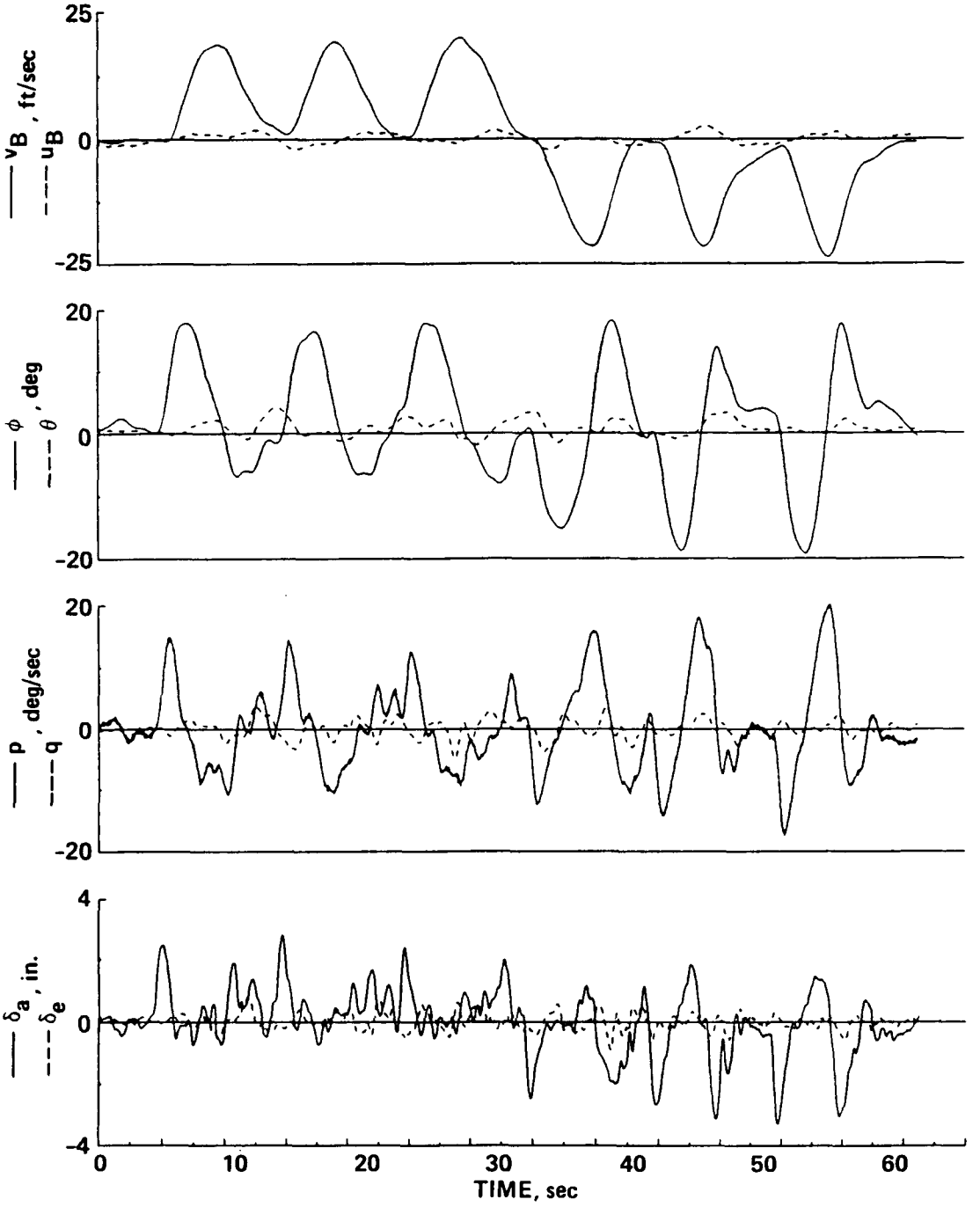

Figure 15 - Time histories from flight data, sidestep task, decoupled model.

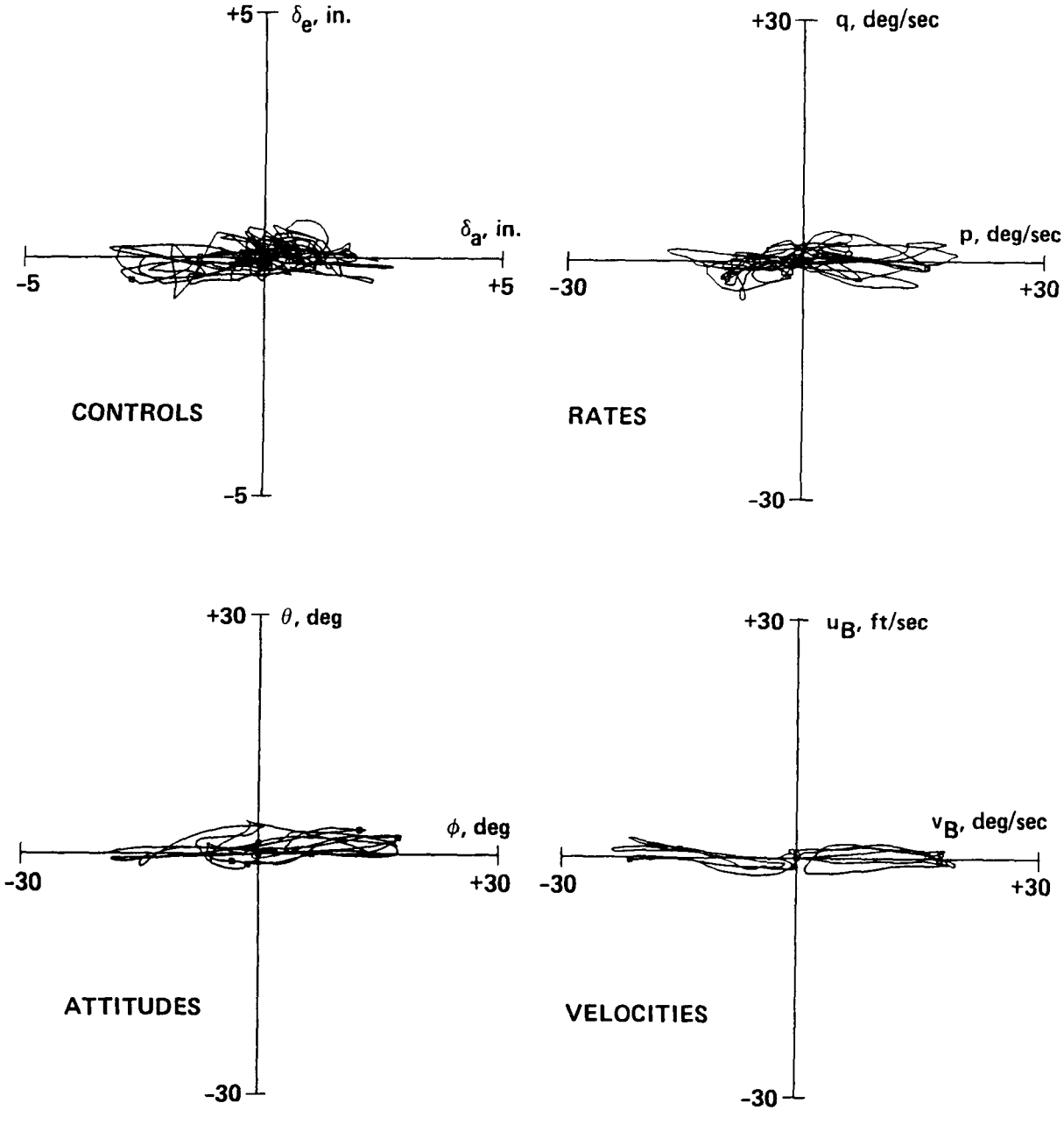

Figure 16 - Crossplots from flight data, sidestep task, decoupled model.

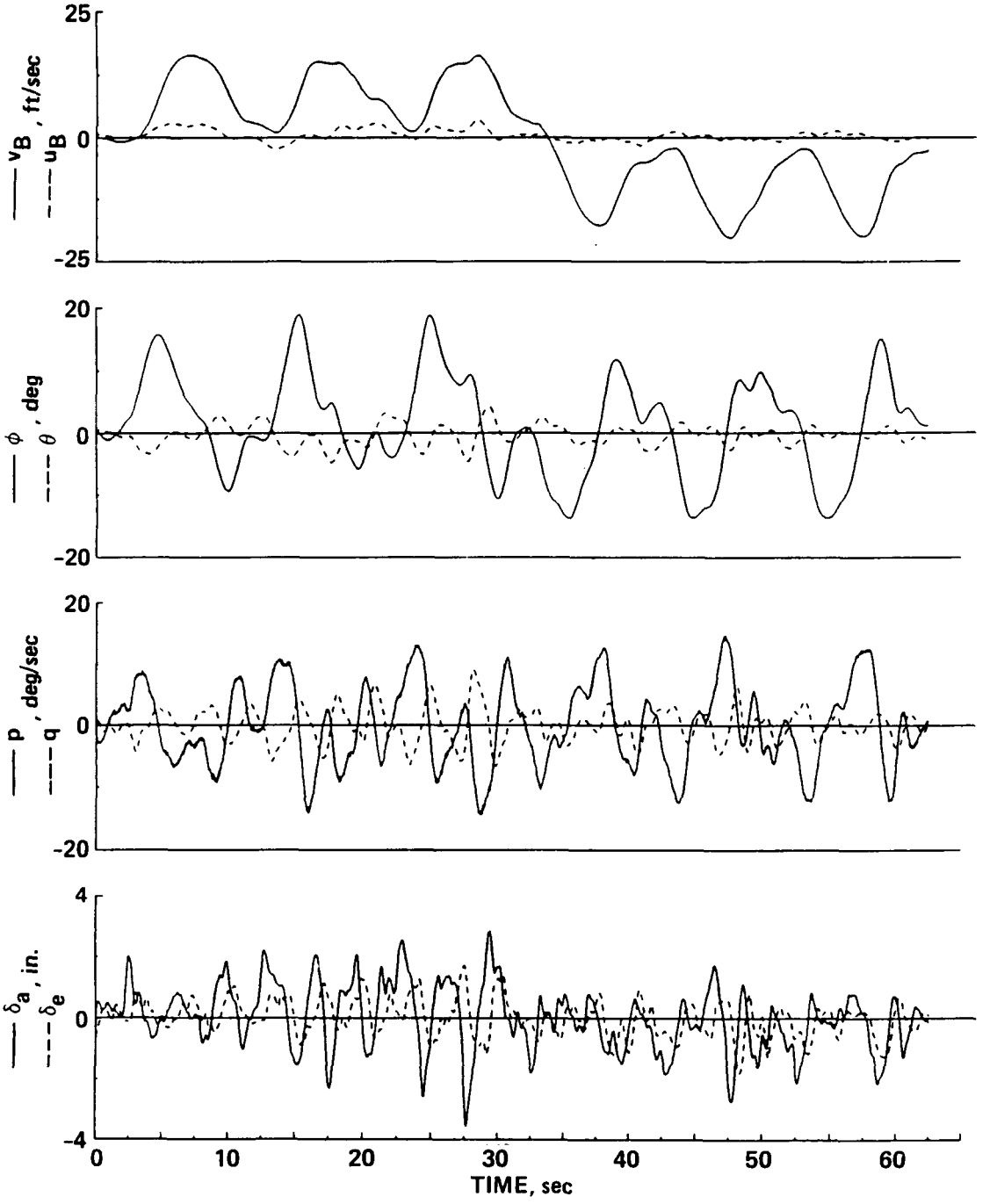

Figure 17 - Time histories from flight data, sidestep task, 45° control coupling.

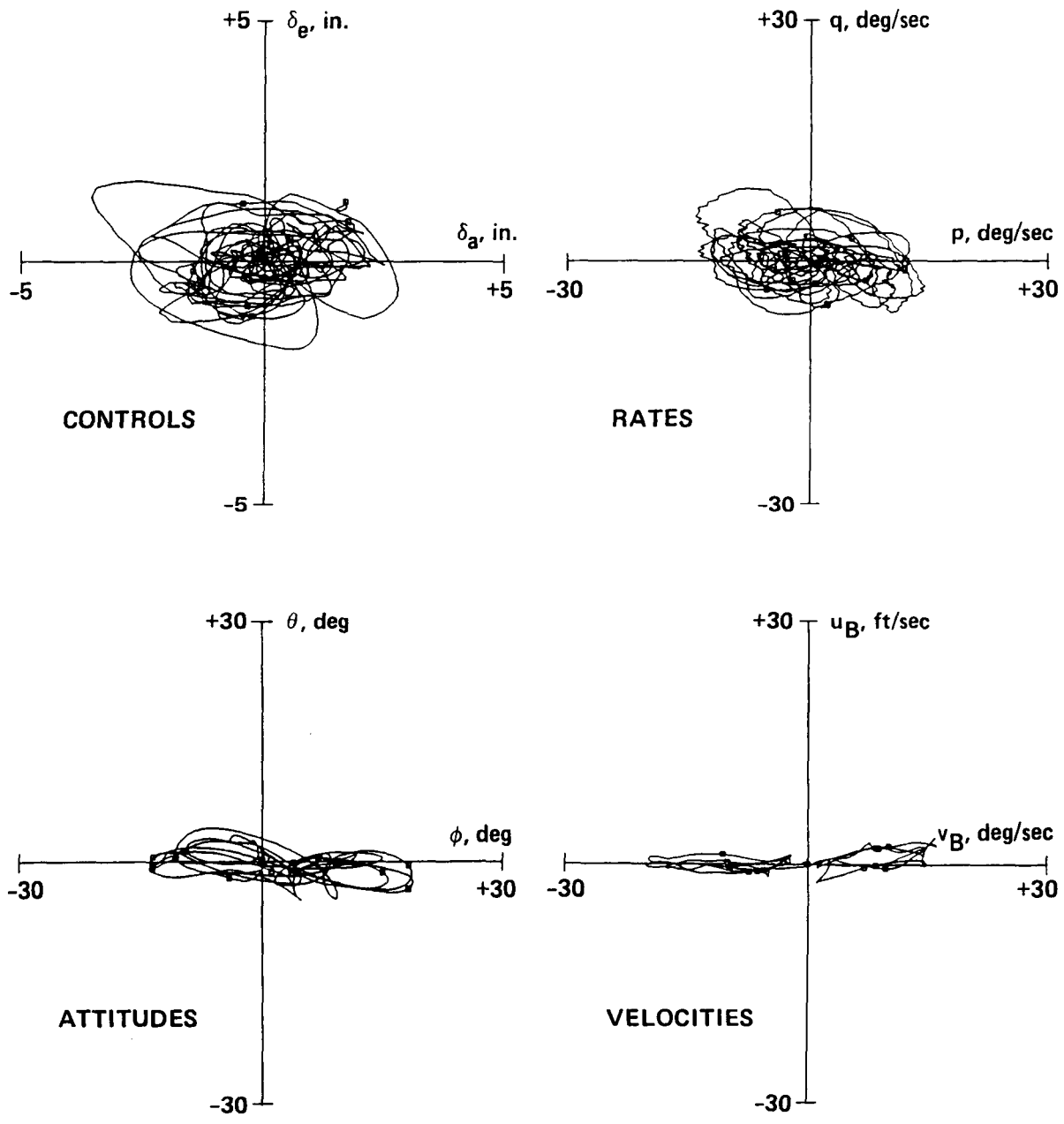

Figure 18 - Crossplots from flight data, sidestep task, 45° control coupling.

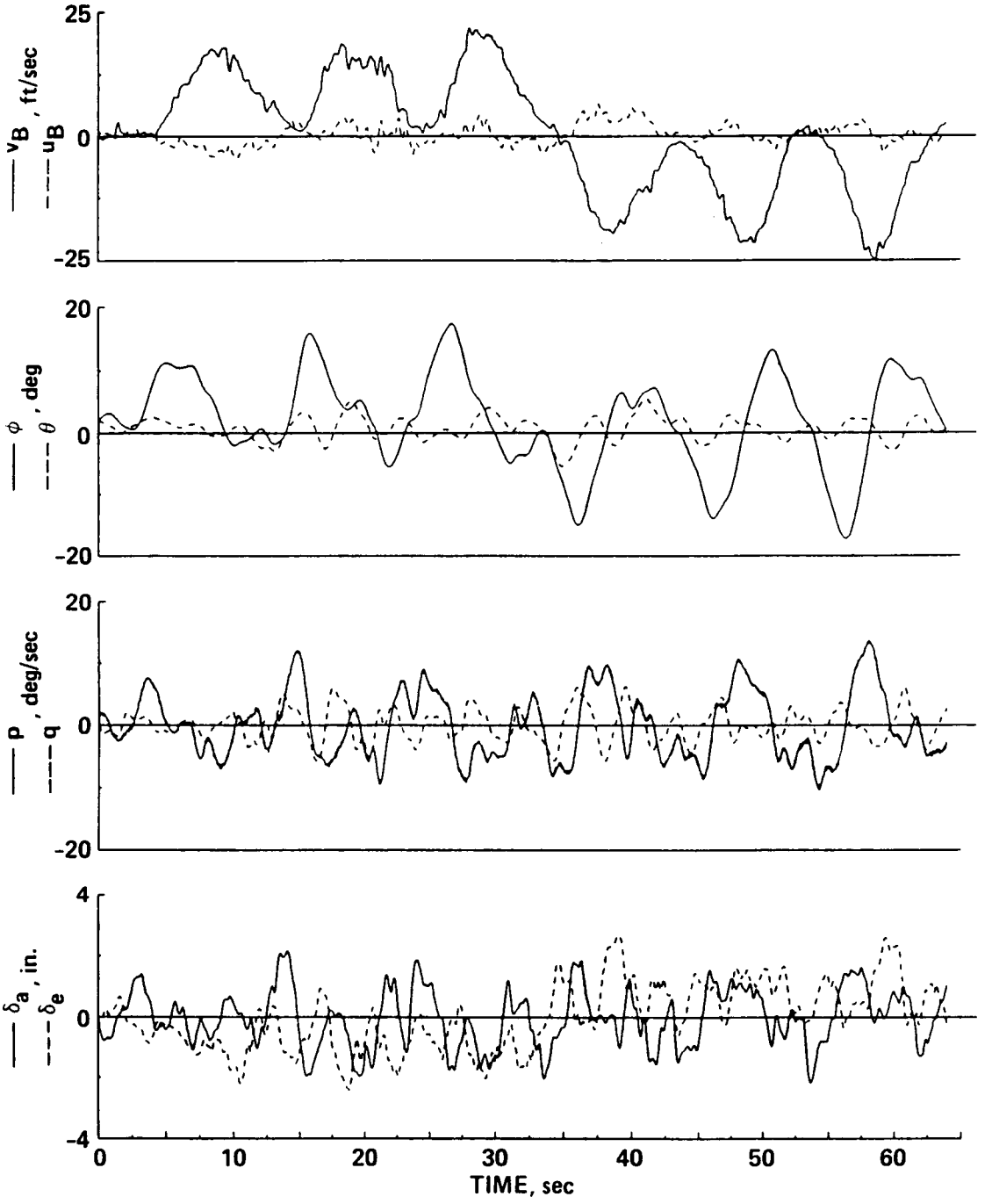

Figure 19 - Time histories from flight data, sidestep task, angular-rate coupling ($| M_p/M_q |= 1.10$).

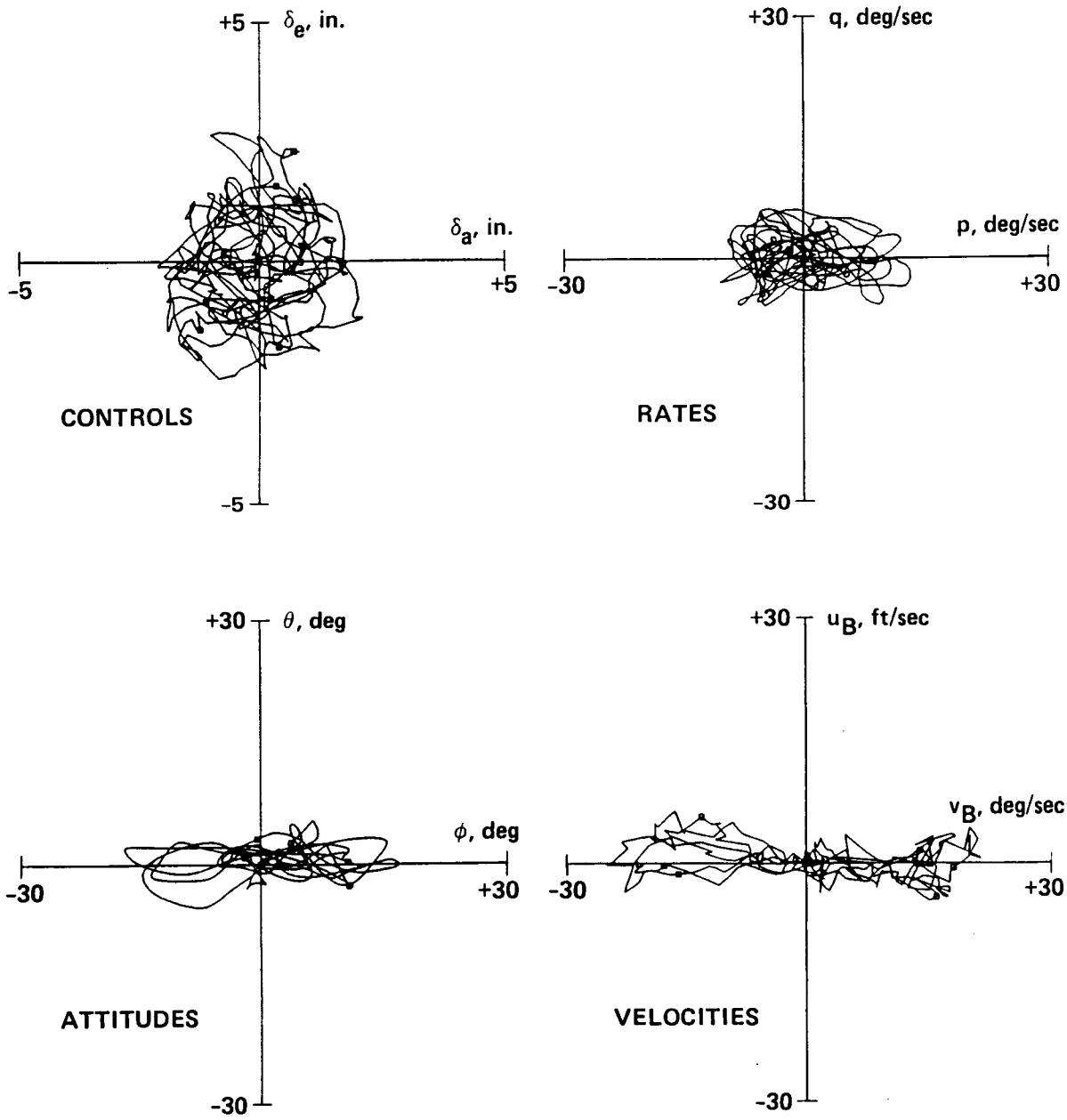

Figure 20 - Crossplots from flight data, sidestep task, angular-rate coupling ($| M_p/M_q |= 1.10$).

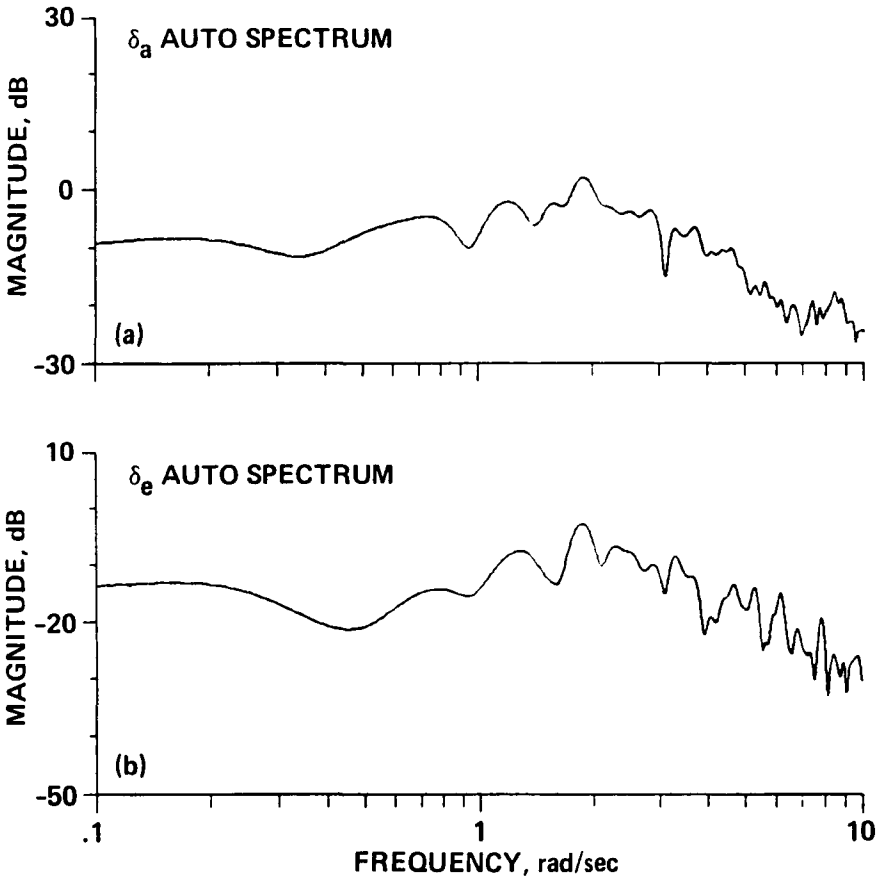

Figure 21 - Lateral and longitudinal control frequency content auto-spectrums, sidestep task, 45° control coupling.

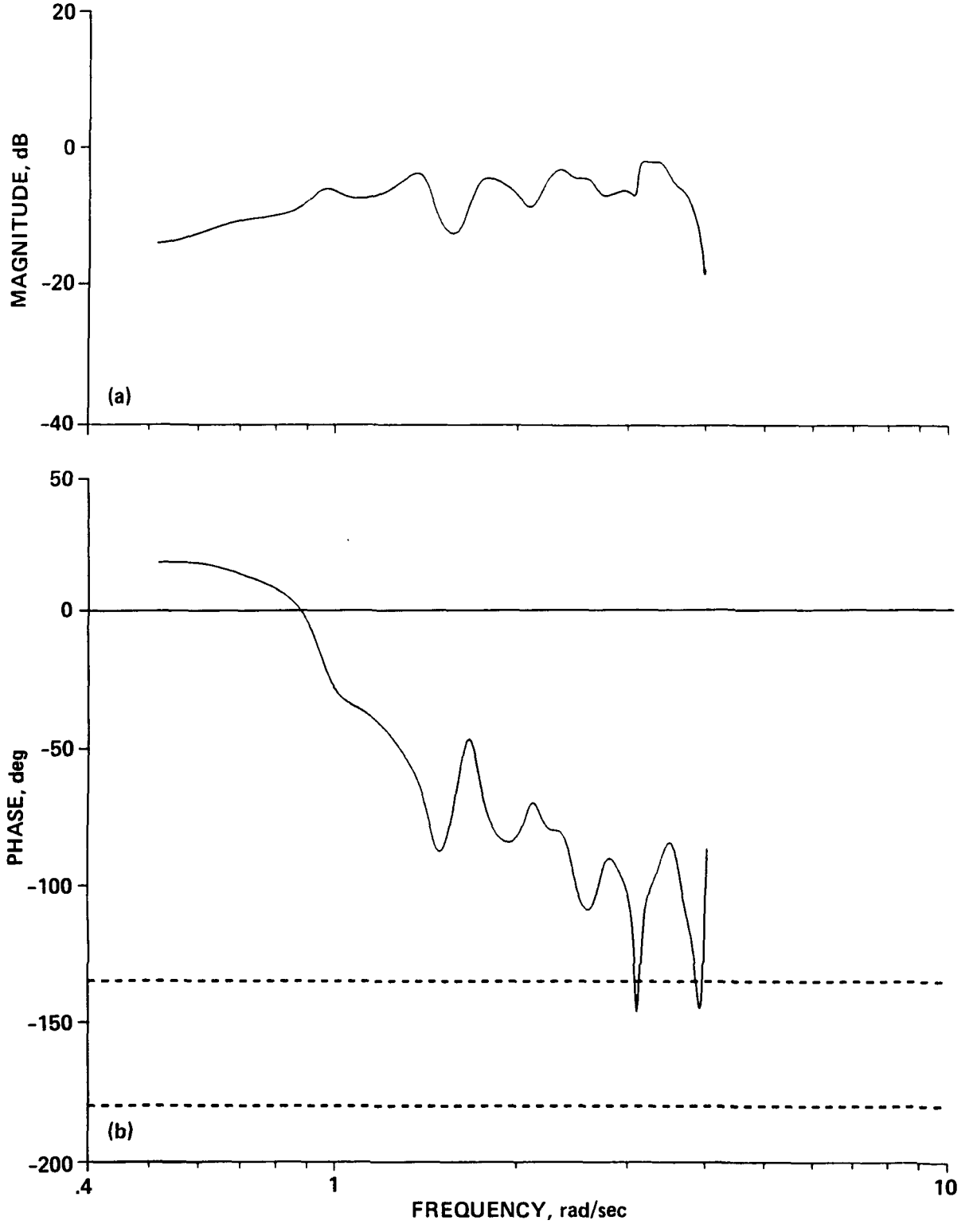

Figure 22 - δ_e/δ_a cross-control magnitude and phase, sidestep task, 45° control coupling.

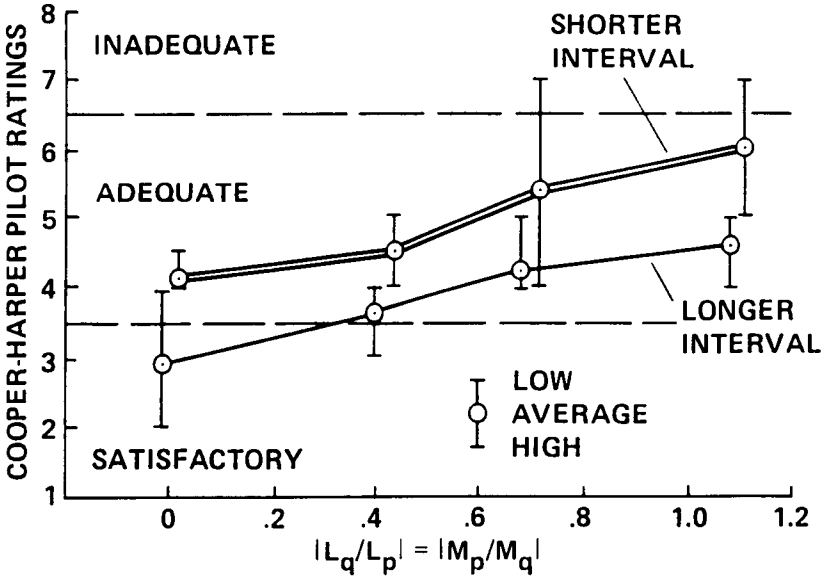

Figure 23 - Pilot ratings from the sidestep task in flight, angular-rate coupling.

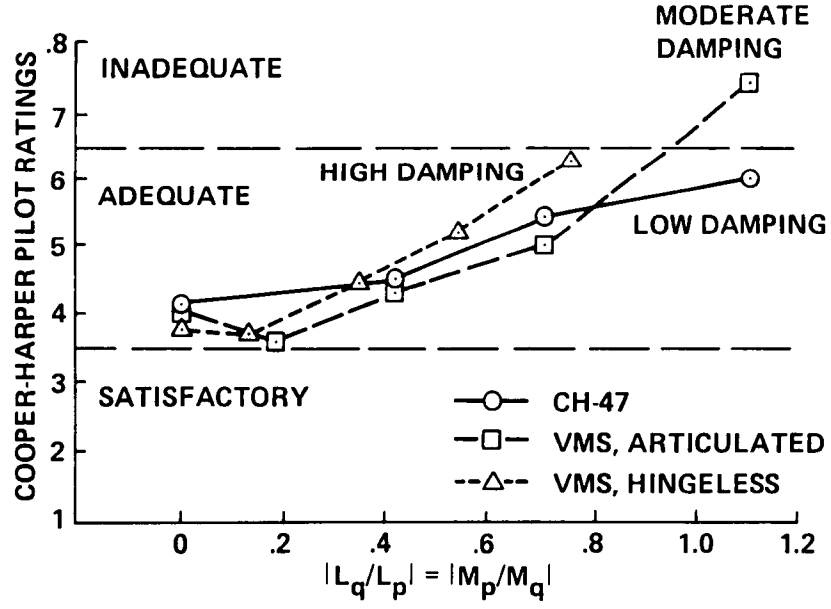

Figure 24 - Comparison of pilot ratings from flight and simulation, sidestep task, angular-rate coupling.

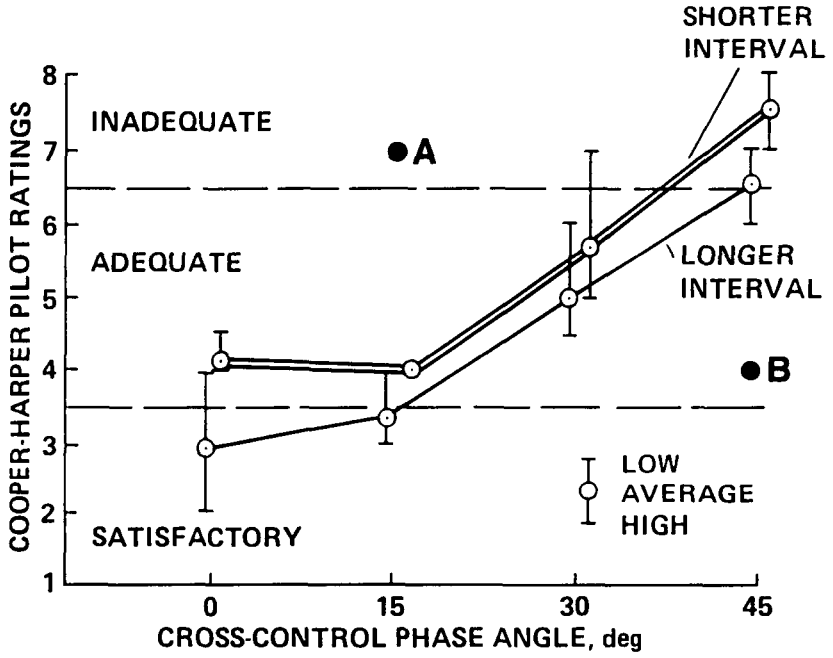

Figure 25 - Pilot ratings from the sidestep task in flight, control coupling.

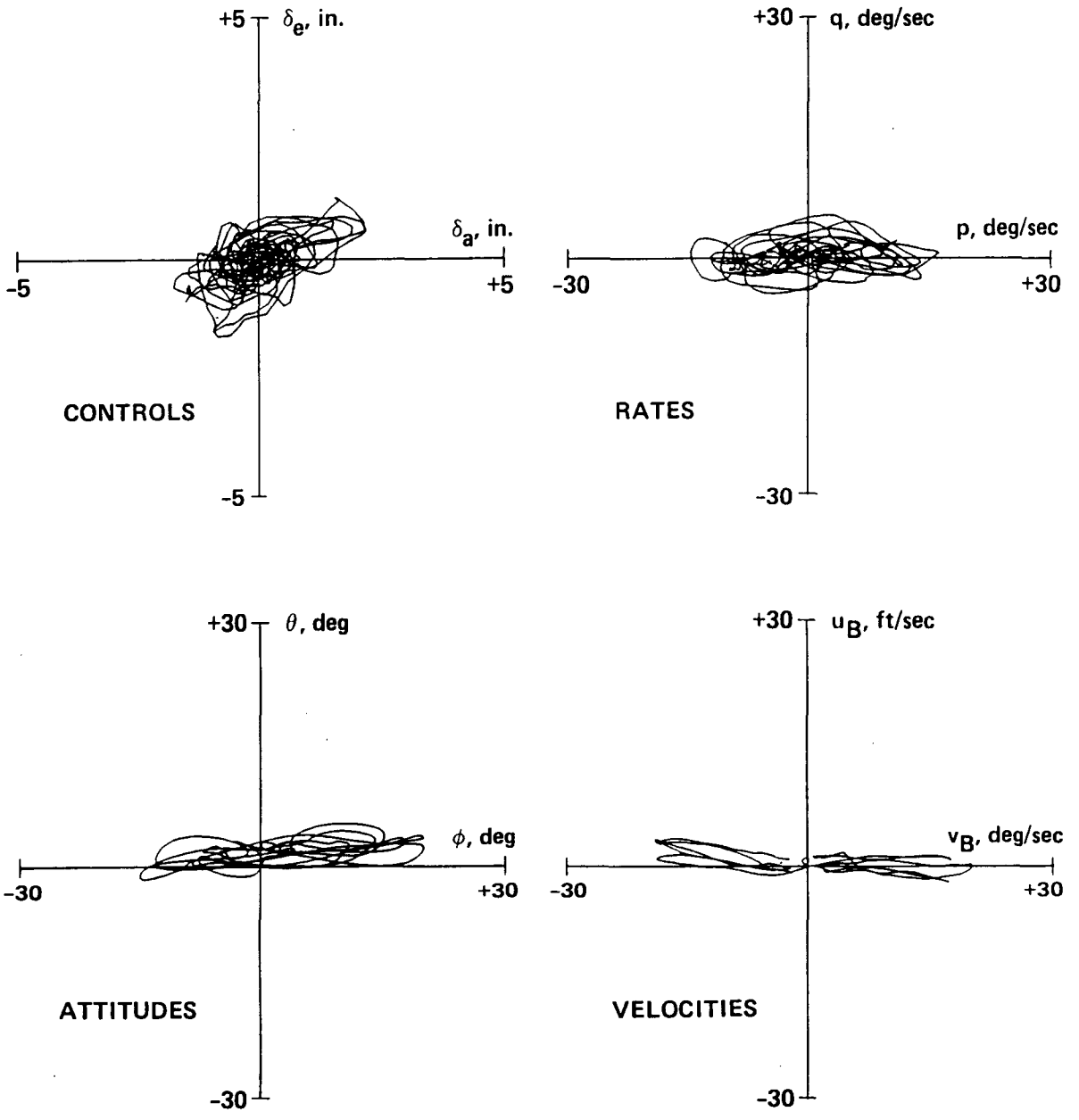

Figure 26 - Crossplots from flight data corresponding to point B, 45° control coupling, longer timing, pilot rating = 4.

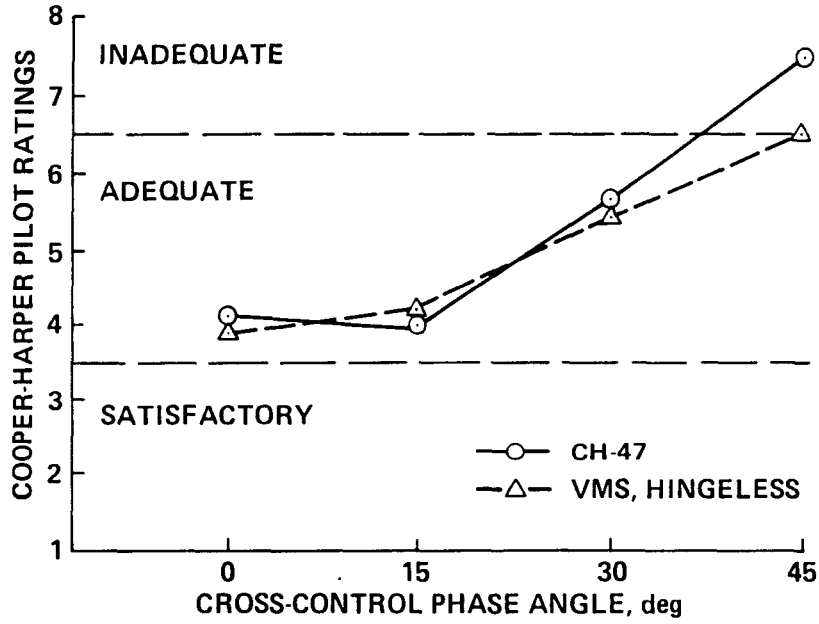

Figure 27 - Comparison of pilot ratings from flight and simulation, sidestep task, control coupling.

NASA
National Aeronautics and Space Administration

Report Documentation Page

1. Report No.	2. Government Accession No.	3. Recipient's Catalog No.
NASA TM-101059		

4. Title and Subtitle	5. Report Date
In-Flight Simulation Investigation of Rotorcraft Pitch-Roll Cross Coupling	December 1988
	6. Performing Organization Code

7. Author(s)	8. Performing Organization Report No.
Douglas C. Watson and William S. Hindson	A-89016
	10. Work Unit No. 505-66-51

9. Performing Organization Name and Address	11. Contract or Grant No.
Ames Research Center Moffett Field, CA 94035	
	13. Type of Report and Period Covered
12. Sponsoring Agency Name and Address	Technical Memorandum
National Aeronautics and Space Administration Washington, DC 20546-0001	14. Sponsoring Agency Code

15. Supplementary Notes

Point of Contact: Douglas C. Watson, Ames Research Center, MS 211-2, Moffett Field, CA 94035
(415) 694-4037 or FTS 464-4037

16. Abstract

An in-flight simulation experiment investigating the handling qualities effects of pitch-roll cross-coupling characteristic of single-main-rotor helicopters is described The experiment was conducted using the NASA/Army CH-47B variable stability helicopter with an explicit-model-following control system. The research is an extension of an earlier ground-based investigation conducted on the NASA Ames Research Center's Vertical Motion Simulator. The model developed for the experiment is for an unaugmented helicopter with cross-coupling implemented using physical rotor parameters. The details of converting the model from the simulation to use in flight are described. A frequency-domain comparison of the model and actual aircraft responses showing the the fidelity of the in-flight simulation is described. the evaluation task was representative of nap-of-the-Earth maneuvering flight. the results indicate that task demands are important in determining allowable levels of coupling. In addition, on-axis damping characteristics influence the frequency-dependent characteristics of coupling and affect the handling qualities. Pilot technique, in terms of learned control crossfeeds, can improve performance and lower workload for particular types of coupling. The results obtained in flight corroborated the simulation results.

17. Key Words (Suggested by Author(s))	18. Distribution Statement
In-flight simulation Cross coupling Handling qualities	Unclassified-Unlimited Subject Category – 08

19. Security Classif. (of this report)	20. Security Classif. (of this page)	21. No. of pages	22. Price
Unclassified	Unclassified	41	A03